Table 1 The unique amino acid substitutions in strain HBDI03 in comparison with eight previously isolated genotype H hepatitis B virus strains

Amino acid position	Consensus residue of genotype H	Residue unique to strain HBDI03
Polymerase		
519 (rt173)	V	L/V
526 (rt180)	L	M
548 (rt202)	S	G/S
550 (rt204)	M	V
Surface		
164	E	D/E
195	I	M
X		
32	W	G

Consensus residues of genotype H were from the eight reported hepatitis B virus (HBV) strains (GenBank accession nos. AY090454, AY090457, AY090460, AP007261, AB179747, AB205010, AB266536 and AB298362).

changes. As for the remaining one amino acid substitution in the X gene, the substituted glycine residue observed in the HBDI03 strain was a common one in the representative HBV strains of genotypes A–G at the corresponding codon position. Taken together, the HBDI03 strain did not appear to have any distinctive features other than the presence of the drug-associated amino acid substitutions.

DISCUSSION

RECENTLY, ETV HAS been widely accepted as an effective drug for the treatment of HBV monoinfection because of its stronger inhibitory effect on HBV replication and lower emergence rate of drug-resistant mutant virus compared to LAM.[12–14] ETV-resistant HBV has been demonstrated to be established by amino acid substitution(s) at rt184, rt202 and/or rt250, in addition to the LAM-resistant rtM204V/I and rtL180M substitutions.[15] The emergence rate of ETV-resistant virus has been reported to be higher in LAM-resistant patients than in naïve patients.[16] There has so far been little evidence concerning the anti-HBV efficacy of ETV for patients with HBV/HIV coinfection. In particular, LAM-resistant HBV has been shown to emerge frequently in patients with HBV/HIV coinfection who received LAM therapy as a component of HAART.[7] The therapeutic efficacy of ETV on LAM-resistant HBV should be assessed in patients with HBV/HIV coinfection. In this study, we examined a patient with HBV/HIV coinfection who had LAM-resistant HBV induced by HAART including LAM, and underwent subsequent ETV therapy. The patient showed a rather weak suppressive effect of ETV on HBV replication, followed by the emergence of ETV-resistant HBV in the early phase of therapy.

In the sequence analysis of the HBV genome, no drug-resistant HBV mutations were detected before HAART, but continuous LAM administration induced the LAM-resistant mutant HBV with rtM204V, rtL180M and rtV173L amino acid substitutions. Subsequent ETV therapy resulted in the emergence of an ETV-resistant virus possessing the rtS202G substitution in addition to the three LAM resistance-associated substitutions after no more than 6 months of ETV therapy, although the rtS202G and rtV173L substitutions were incomplete. In LAM-resistant patients with HBV monoinfection, the emergence rate of the ETV-resistant mutation has been reported to be merely 15% after 3 years of therapy.[16] In comparison with this, ETV-resistant HBV appeared in an extremely early phase of therapy in our patient with HBV/HIV coinfection. According to this, ETV resistance is speculated to be established earlier in patients with HBV/HIV coinfection than in those with HBV monoinfection, although concomitant HIV infection has not thus far been suggested to result in a higher incidence of the drug-resistant HBV strain in the treatment with other anti-HBV drugs in chronic HBV infection. The latent immune deficiency caused by HIV infection might prevent HBV eradication through a host immune response, resulting in poor anti-HBV efficacy of ETV. Alternatively, simultaneous usage of multiple antiretroviral drugs might in some way contribute to the emergence of ETV-resistant HBV.

Very recently, it has been shown that ETV possesses modest anti-HIV activity both *in vitro* and *in vivo* and can induce the drug-resistant mutant HIV strain in patients with HBV/HIV coinfection.[18] This suggests that ETV may not be appropriate for the treatment of patients with HBV/HIV coinfection in whom HAART is not needed. On the other hand, ETV is considered to be beneficial for patients with HBV/HIV coinfection undergoing a stable continuation of HAART. In particular, the therapeutic efficacy of ETV may be more promising in patients without LAM-resistant HBV than in those with it. Although the present case of the patient under discussion, who already displayed LAM-resistant HBV due to the preceding HAART, did not support the usefulness of ETV therapy because of the early emergence of ETV-resistant HBV, further studies with a large number of

patients should be completed to assess the antiviral efficacy and deliberate clinical application of ETV therapy for HBV/HIV coinfection.

Both adefovir dipivoxil (ADV) and tenofovir disoproxil fumarate (TDF) have recently been shown to effectively inhibit HBV replication in patients with HBV/HIV coinfection, irrespective of LAM resistance.[19,20] ADV exerts only anti-HBV activity and is available for patients with HBV/HIV coinfection who have no need for HAART or who are receiving a stable HAART regimen. In contrast, TDF can be used as a component of HAART because of its valuable antiviral activity against both HBV and HIV. Accordingly, ADV and TDF are currently useful drugs for patients with HBV/HIV coinfection and may be subsequent therapeutic options for the patient reported in this study.

Our patient was found to be infected with HBV of genotype H, a globally rare genotype. To date, the full-length sequences of eight genotype H HBV strains have been reported from the USA, Nicaragua and Japan (see Fig. 2). Of them, one strain has been obtained from a Japanese patient with chronic HBV monoinfection who underwent ETV therapy as a naïve patient and showed ETV resistance later.[21] The relevance of the genotype frequency to the therapeutic efficacy of ETV should be studied extensively in HBV-infected patients treated with ETV.

In Japan, genotypes B and C are prevalent in chronic HBV carriers who acquire the infection mainly through the mother-to-child transmission route. In contrast, the foreign HBV strains other than genotypes B and C have been shown to be involved in a considerable proportion of patients with acute HBV infection.[22] Infection of such foreign types of HBV possibly occurs through sexual contacts in Japan. In our patient with HBV/HIV coinfection who had genotype H HBV of foreign origin, it is speculated that acute HBV infection occurring 3 years before his first visit led to the transition to chronicity. The time of HIV infection cannot be defined due to the lack of HIV-RNA testing during the period of acute HBV infection. The possibility of simultaneous infection with HBV and HIV cannot be excluded, despite the negative result of anti-HIV at that time, because the test may have taken place during the immunological window period of HIV infection.

In summary, we have introduced a patient with HBV/HIV coinfection who underwent ETV therapy in addition to the HAART regimen and showed ETV resistance in the early phase of therapy. Our finding suggests that, in ETV therapy for patients with HBV/HIV infection, great care should be taken against the emergence of ETV-resistant HBV, especially in patients with pre-existing LAM-resistant HBV.

REFERENCES

1 Lee WM. Hepatitis B virus infection. *N Engl J Med* 1997; 337: 1733–45.
2 Konopnicki D, Mocroft A, de Wit S *et al.* EuroSIDA Group. Hepatitis B and HIV: prevalence, AIDS progression, response to highly active antiretroviral therapy and increased mortality in the EuroSIDA cohort. *AIDS* 2005; 19: 593–601.
3 Thio CL, Seaberg EC, Skolasky R Jr *et al.* Multicenter AIDS Cohort Study. HIV-1, hepatitis B virus, and risk of liver-related mortality in the Multicenter Cohort Study (MACS). *Lancet* 2002; 360: 1921–6.
4 Lai CL, Chien RN, Leung NW *et al.* A one-year trial of lamivudine for chronic hepatitis B. Asia Hepatitis Lamivudine Study Group. *N Engl J Med* 1998; 339: 61–8.
5 Benhamou Y, Katlama C, Lunel F *et al.* Effects of lamivudine on replication of hepatitis B virus in HIV-infected men. *Ann Intern Med* 1996; 125: 705–12.
6 Lai CL, Dienstag J, Schiff E *et al.* Prevalence and clinical correlates of YMDD variants during lamivudine therapy for patients with chronic hepatitis B. *Clin Infect Dis* 2003; 36: 687–96.
7 Benhamou Y, Bochet M, Thibault V *et al.* Long-term incidence of hepatitis B virus resistance to lamivudine in human immunodeficiency virus-infected patients. *Hepatology* 1999; 30: 1302–6.
8 Allen MI, Deslauriers M, Andrews CW *et al.* Identification and characterization of mutations in hepatitis B virus resistant to lamivudine. Lamivudine Clinical Investigation Group. *Hepatology* 1998; 27: 1670–7.
9 Ono-Nita SK, Kato N, Shiratori Y *et al.* Susceptibility of lamivudine-resistant hepatitis B virus to other reverse transcriptase inhibitors. *J Clin Invest* 1999; 103: 1635–40.
10 Ono SK, Kato N, Shiratori Y *et al.* The polymerase L528M mutation cooperates with nucleotide binding-site mutations, increasing hepatitis B virus replication and drug resistance. *J Clin Invest* 2001; 107: 449–55.
11 Delaney WE, Yang H, Westland CE *et al.* The hepatitis B virus polymerase mutation rtV173L is selected during lamivudine therapy and enhances viral replication in vitro. *J Virol* 2003; 77: 11833–41.
12 Chang TT, Gish RG, de Man R *et al.* BEHoLD AI463022 Study Group. A comparison of entecavir and lamivudine for HBeAg-positive chronic hepatitis B. *N Engl J Med* 2006; 354: 1001–10.
13 Lai CL, Shouval D, Lok AS *et al.* BEHoLD AI463027 Study Group. Entecavir versus lamivudine for patients with HBeAg-negative chronic hepatitis B. *N Engl J Med* 2006; 354: 1011–20.
14 Sherman M, Yurdaydin C, Sollano J *et al.* AI463026 BEHoLD Study Group. Entecavir for treatment of

lamivudine-refractory, HBeAg-positive chronic hepatitis B. *Gastroenterology* 2006; **130**: 2039–49.
15 Tenney DJ, Rose RE, Baldick CJ *et al.* Two-year assessment of entecavir resistance in Lamivudine-refractory hepatitis B virus patients reveals different clinical outcomes depending on the resistance substitutions present. *Antimicrob Agents Chemother* 2007; **51**: 902–11.
16 Colonno RJ, Rose R, Pokornowski K *et al.* Assessment at three years shows barrier to resistance is maintained in entecavir-treated nucleoside-naïve patients while resistance emergence increases over time in lamivudine refractory patients. *Hepatology* 2007; **44**: 229A (Abstract).
17 Kanada A, Takehara T, Ohkawa K *et al.* Type B fulminant hepatitis is closely associated with a highly mutated hepatitis B virus strain. *Intervirology* 2007; **50**: 394–401.
18 McMahon MA, Jilek BL, Brennan TP *et al.* The HBV drug entecavir – Effects on HIV-1 replication and resistance. *N Engl J Med* 2007; **356**: 2614–21.
19 Benhamou Y, Thibault V, Vig P *et al.* Safety and efficacy of adefovir dipivoxil in patients infected with lamivudine-resistant hepatitis B and HIV-1. *J Hepatol* 2006; **44**: 62–7.
20 Benhamou Y, Fleury H, Trimoulet P *et al.* TECOVIR Study Group. Anti-hepatitis B virus efficacy of tenofovir disoproxil fumarate in HIV-infected patients. *Hepatology* 2006; **43**: 548–55.
21 Suzuki F, Akuta N, Suzuki Y *et al.* Selection of a virus strain resistant to entecavir in a nucleoside-naïve patient with hepatitis B of genotype H. *J Clin Virol* 2007; **39**: 149–52.
22 Ozasa A, Tanaka Y, Orito E *et al.* Influence of genotypes and precore mutations on fulminant or chronic outcome of acute hepatitis B virus infection. *Hepatology* 2006; **44**: 326–34.

JOURNAL OF VIROLOGY, Jan. 2008, p. 196–206
0022-538X/08/$08.00+0 doi:10.1128/JVI.01640-07

Vol. 82, No. 1

Lymphocytoid Choriomeningitis Virus Activates Plasmacytoid Dendritic Cells and Induces a Cytotoxic T-Cell Response via MyD88▽

Andreas Jung,[1,2] Hiroki Kato,[1] Yutaro Kumagai,[1] Himanshu Kumar,[1] Taro Kawai,[1,3] Osamu Takeuchi,[1,3] and Shizuo Akira[1,3]*

Research Institute for Microbial Diseases, Department of Host Defense, Osaka University, Osaka, Japan[1]; Department of Neonatology, Campus Mitte, Charité-Universitaetsmedizin Berlin, Berlin, Germany[2]; and ERATO, Japan Science and Technology Agency, Osaka, Japan[3]

Received 26 July 2007/Accepted 4 October 2007

Toll-like receptors (TLRs) and retinoic acid-inducible gene I-like helicases (RLHs) are two major machineries recognizing RNA virus infection of innate immune cells. Intracellular signaling for TLRs and RLHs is mediated by their cytoplasmic adaptors, i.e., MyD88 or TRIF and IPS-1, respectively. In the present study, we investigated the contributions of TLRs and RLHs to the cytotoxic T-lymphocyte (CTL) response by using lymphocytoid choriomeningitis virus (LCMV) as a model virus. The generation of virus-specific cytotoxic T lymphocytes was critically dependent on MyD88 but not on IPS-1. Type I interferons (IFNs) are known to be important for the development of the CTL response to LCMV infection. Serum levels of type I IFNs and proinflammatory cytokines were mainly dependent on the presence of MyD88, although IPS-1$^{-/-}$ mice showed a decrease in IFN-α levels but not in IFN-β and proinflammatory cytokine levels. Analysis of *Ifna6*$^{+/GFP}$ reporter mice revealed that plasmacytoid dendritic cells (DCs) are the major source of IFN-α in LCMV infection. MyD88$^{-/-}$ mice were highly susceptible to LCMV infection in vivo. These results suggest that recognition of LCMV by plasmacytoid DCs via TLRs is responsible for the production of type I IFNs in vivo. Furthermore, the activation of a MyD88-dependent innate mechanism induces a CTL response, which eventually leads to virus elimination.

Viral infections are initially recognized by the innate immune system, which eliminates invading viruses by itself and activates an antigen-specific acquired immune response (2, 4, 17). Type I interferons (IFNs) are produced by innate immune cells after virus infection and play a pivotal role in antiviral responses, including apoptosis of virus-infected cells, cellular resistance to viral infection, and activation of natural killer and T cells (15, 25, 34). The expression of type I IFN genes is controlled by intracellular signaling pathways triggered by recognition of viral components with innate pattern recognition receptors. Toll-like receptors (TLRs) and retinoic acid-inducible gene I (RIG-I)-like helicases (RLHs), also called RIG-I-like receptors, are two major receptor families responsible for initial viral recognition (20, 28).

TLRs are type I transmembrane receptors responsible for the recognition of microbial components. Among TLRs, TLR7 and TLR9 recognize single-stranded RNA and CpG motif-containing DNA, respectively, and play an important role in virus-induced type I IFN production by plasmacytoid dendritic cells (pDCs) (2, 20). MyD88, a cytoplasmic adaptor protein containing a Toll/interleukin-1 receptor (IL-1R) homology (TIR) domain, is essential for TLR/IL-1R signaling. Mice lacking MyD88 do not respond to various TLR ligands, except for TLR3, a receptor which utilizes TIR domain-containing adaptor-inducing IFN-β (TRIF) in its downstream pathway (2, 40). MyD88 forms a complex with IL-1R-associated kinase 1 (IRAK-1), IRAK-4, and IFN regulatory factor 7 (IRF-7) upon ligand stimulation. Phosphorylated IRF-7 finally translocates into the nucleus to upregulate the expression of a set of IFN-inducible genes (38).

RLHs, including RIG-I and melanoma differentiation-associated gene 5 (MDA5), are cytoplasmic proteins responsible for the recognition of viral double-stranded RNA (20, 41, 42). RIG-I and MDA5 are comprised of caspase recruitment domains (CARDs) and an RNA helicase domain. Studies using knockout mice revealed that RIG-I is responsible for the recognition of various RNA viruses, including vesicular stomatitis virus, influenza virus, Japanese encephalitis virus, and paramyxoviruses such as Newcastle disease virus and Sendai virus, whereas MDA5 detects viruses belonging to the picornavirus family, such as encephalomyocarditis virus (11, 18, 19). RIG-I and MDA5 detect double-stranded RNAs via the helicase domain and initiate downstream signaling cascades via the CARDs by associating with a CARD-containing signaling protein named IFN-β promoter stimulator 1 (IPS-1) (also known as MAVS, VISA, or CARDIF) (21, 27, 33, 39). IPS-1 signals through IκB kinase-related kinases, called IKK-*i* and TBK1, that phosphorylate IRF-3/7 to induce the expression of IFN-inducible genes (2). Cells deficient in IPS-1 fail to produce type I IFNs and NF-κB-dependent proinflammatory cytokines in response to infection with different families of RNA viruses recognized by RIG-I and MDA5 (24, 35). The RLH signaling pathway is critical for type I IFN production in various cell types, including conventional DCs (cDCs), fibroblasts, and

* Corresponding author. Mailing address: WPI Immunology Frontier Research Center, Laboratory of Host Defense, Osaka University, 3-1 Yamada-oka, Suita 565-0871, Osaka, Japan. Phone: 81-6-6879 8303. Fax: 81-6-6879 8305. E-mail: sakira@biken.osaka-u.ac.jp.

▽ Published ahead of print on 17 October 2007.

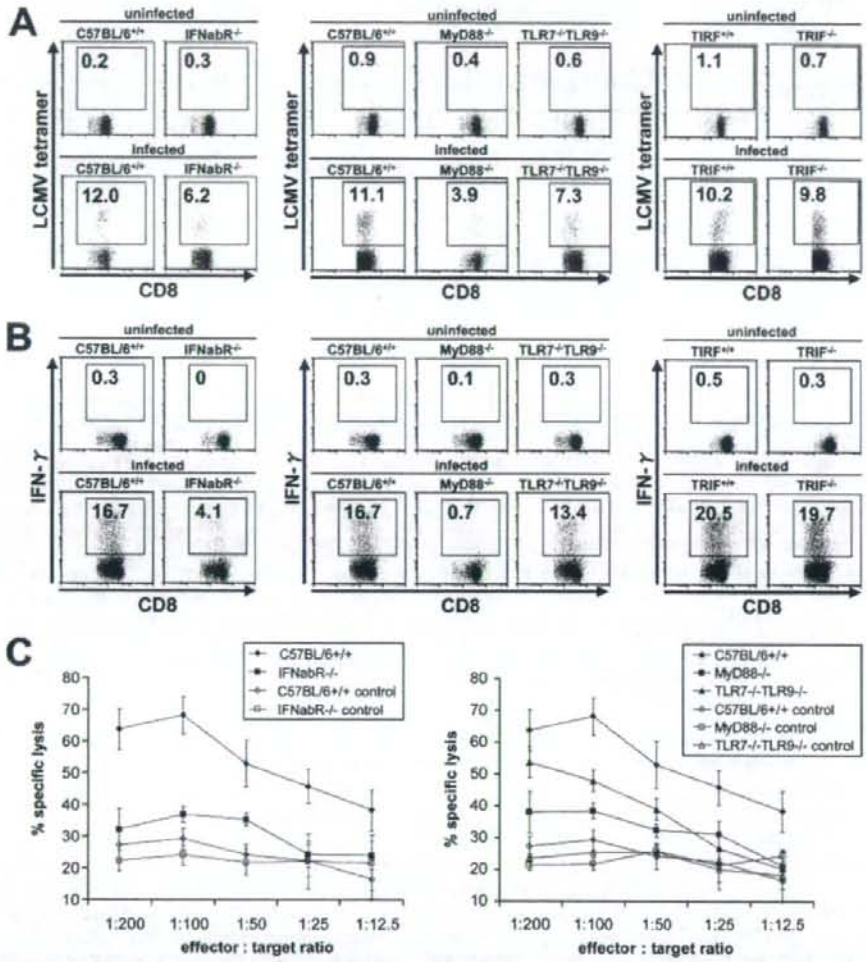

FIG. 1. Induction of LCMV-specific T-cell response via the TLR system. Wild-type, MyD88$^{-/-}$, IFN-α/β receptor$^{-/-}$, TLR7$^{-/-}$ TLR9$^{-/-}$, and TRIF$^{-/-}$ mice were infected intravenously with 3×10^5 PFU LCMV WE, and splenocytes were harvested on day 8 after infection. Cells were stained with LCMV major histocompatibility complex class I tetramer, CD4, and CD8α antibodies (A) or stimulated with gp33-41 prior to CD8α antibody staining (B). Induction of LCMV-specific T lymphocytes and IFN-γ production was analyzed by flow cytometry. (C) Ex vivo CTL activity in splenocytes was determined by a 5-h ^{51}Cr release assay, using gp33-41-loaded EL4 cells as targets. Values are means ± standard deviations (SD) for three mice. Data are representative of three independent experiments.

macrophages, but not in pDCs (23, 24). Thus, both the TLR system and the RLH system participate in virus recognition as well as signal transduction leading to IFN induction. However, the exact mechanisms by which TLRs and RLHs are involved in the development of acquired immune responses have yet to be clarified.

Lymphocytoid choriomeningitis virus (LCMV) is an ambisense single-stranded RNA virus belonging to the family *Arenaviridae*. Numerous strains of this noncytolytic pathogen, such as WE and Armstrong 53b (ARM), cause acute infections in mice, whereas rapidly replicating immunosuppressive variants lead to virus persistence and a general immunosuppression (30). Nonimmunosuppressive LCMV infections result in a profound adaptive immune response that is highlighted by the generation of virus-specific CD4$^+$ and CD8$^+$ T lymphocytes. Activated T cells acquire effector functions, such as IFN-γ production and cytolytic activity, that are responsible for clearing the virus, usually within 7 to 15 days after infection, and eventually lead to a functional T-cell memory (32). Initiation of this specific T-lymphocyte induction is considered to rely on antigen-presenting cells, mainly CD8α$^+$ DCs (3). After capturing the viral antigen, the DCs migrate to lymphoid organs, such as the spleen, where they activate naïve T cells (12). In this process, type I IFNs are believed to play a central role in controlling viral infections such as LCMV infection. They have been shown to act directly on T lymphocytes and to induce

massive expansion of antigen-specific CD8$^+$ T cells (1, 7, 22, 32).

Nevertheless, the source of type I IFN in response to LCMV remains controversial, and type I IFN-producing cells are not well characterized. pDCs have been shown to be a major source of type I IFNs in various murine virus infections (6, 8, 9). pDCs were also implicated as the source of IFN-α in the LCMV-infected spleen (29). Conversely, it was reported that production of type I IFNs in response to LCMV infection was not impaired in pDC-depleted mice, questioning the importance of pDCs in T-cell induction in response to LCMV (8). Furthermore, cDCs extracted from mice infected with LCMV were reported to produce high IFN-α levels (10).

In the present study, we investigated the involvement of TLRs and RLHs in the development of antigen-specific CD8$^+$ T cells as well as in the production of type I IFNs in response to LCMV infection by using MyD88-deficient (MyD88$^{-/-}$) and IPS-1$^{-/-}$ mice. The development of cytotoxic T lymphocytes (CTLs) was critically dependent on MyD88 but not on IPS-1. MyD88-deficient mice were revealed to be highly susceptible to LCMV infection. In contrast to previous reports, levels of IFN-α, IFN-β, and proinflammatory cytokines in sera were dependent on the presence of MyD88, whereas IPS-1 deficiency resulted in impaired IFN-α production but otherwise normal cytokine levels. pDCs were the major source of IFN-α in LCMV infection. These results suggest that LCMV activates pDCs via TLRs to produce type I IFNs in vivo and that the activation of an innate mechanism leads to the induction of the CTL response and, eventually, virus elimination.

MATERIALS AND METHODS

Mice. IFN-α/β receptor$^{-/-}$, MyD88$^{-/-}$, TRIF$^{-/-}$, TLR2$^{-/-}$, TLR4$^{-/-}$, TLR8$^{-/-}$, and IPS-1$^{-/-}$ mice have been described previously (14, 16, 24, 36, 40). TLR7$^{-/-}$ and TLR9$^{-/-}$ mice were crossed to yield double TLR7- and TLR9-deficient mice (13, 14). *Ifna6*$^{+/GFP}$ mice were generated as recently described (23).

LCMV infection and virus titration. LCMV WE and ARM were obtained from T. Otheki (31). For virus propagation, L cells were infected with LCMV and cultured at 37°C for 48 h. Supernatants were diluted in phosphate-buffered saline for infection. Mice were infected intravenously with 3×10^5 PFU LCMV strain WE or ARM after a brief anesthesia with diethyl ether. For analysis of survival rates, mice were infected with 2×10^6 PFU. Virus loads in the spleen and liver were investigated on days 4, 8, and 30 after infection. For virus titration, MC57G cells were inoculated with 10-fold serial dilutions of LCMV-containing supernatants in a 24-well plate, covered with 2% methylcellulose, and incubated at 37°C for 48 h. Cells were then fixed with 4% formalin, permeabilized with 0.5% Triton X, and incubated with 10% fetal bovine serum. After subsequent incubation with murine LCMV immunoglobulin G1 (IgG1; Progen Biotechnik) and anti-mouse IgG–horseradish peroxidase (Amersham Biosciences), plates were stained using an AEC peroxidase substrate kit (Vector Laboratories), and virus plaques were counted for each well.

Induction of specific T-cell response. Splenocytes were harvested 8 days after infection. To investigate the activation of LCMV-specific T lymphocytes, cells were incubated with T-select H-2D^b LCMV tetramer-KAVYNFATC-phycoerythrin (PE) (MBL), CD4-fluorescein isothiocyanate (CD4-FITC), and CD8α-allophycocyanin antibodies (BD Pharmingen). Samples were acquired on a FACSCalibur flow cytometer (BD Biosciences) and analyzed with FlowJo software (TreeStar). IFN-γ induction was analyzed by stimulating splenocytes with an LCMV H-2D^b-binding peptide (glycoprotein 33-41 [gp33-41] [KAVYNFATM]; Peptide Institute) and 10 ng/ml murine IL-2 prior to incubation with CD8α antibodies. Cells were then fixed, stained with IFN-γ–FITC antibodies in Perm-Wash solution (BD Pharmingen) according to the manufacturer's recommendation, and assessed by flow cytometry. For determination of cytotoxicity of LCMV-specific T cells, splenocytes were incubated for 5 h with EL-4 target cells that had been loaded with gp33-41 and labeled with ^{51}Cr. The percentage of specific lysis for each sample was calculated as follows: [(sample release − spontaneous release)/(maximal release − spontaneous release)] × 100. To analyze the generation of LCMV-specific memory T lymphocytes, mice were infected with 1×10^5 PFU LCMV WE, and splenocytes were analyzed for activation of specific T memory cells and IFN-γ induction as described below.

TABLE 1. Total and virus-specific numbers of CD8$^+$ T lymphocytes per spleen for uninfected mice and mice that were intravenously infected with 3×10^5 PFU LCMV WE[a]

Mouse group and genotype	Total CD8$^+$ cells	Specific CD8$^+$ cells	% of total
Uninfected mice			
C57BL/6$^{+/+}$	6.6 ± 2.6	0.03 ± 0.04	0.5
IFNabR$^{-/-}$	5.4 ± 0.3	0.03 ± 0.01	0.6
MyD88$^{-/-}$	7.1 ± 1.1	0.03 ± 0.01	0.4
TLR7$^{-/-}$ TLR9$^{-/-}$	6.7 ± 2.2	0.02 ± 0.02	0.3
Infected mice			
C57BL/6$^{+/+}$	19.7 ± 9.2	2.19 ± 1.04	11.1
IFNabR$^{-/-}$	15.7 ± 4.1	0.99 ± 0.25	6.3
MyD88$^{-/-}$	3.6 ± 0.7	0.16 ± 0.06	4.4
TLR7$^{-/-}$ TLR9$^{-/-}$	13.0 ± 2.7	0.98 ± 0.23	7.5

[a] Splenocytes were harvested on day 8 after infection and stained with LCMV major histocompatibility complex class I tetramer and CD8α antibodies. Cell numbers were counted by flow cytometry. Depicted values are multipliers of 10^6 and indicate means ± standard deviations for nine mice per indicated genotype.

Cytokine and type I IFN production. IL-1β, IL-6, IL-10, IL-12(p40), IL-12(p70), RANTES, and tumor necrosis factor alpha were measured in sera 24 and 48 h after LCMV infection by a multiplex bead-based flow cytometry assay (Bio-Plex cytokine assay; Bio-Rad Laboratories). IFN-α and IFN-β were determined repeatedly between 12 and 96 h by enzyme-linked immunosorbent assay (PBL Biomedical Laboratories).

Expression of green fluorescent protein (GFP) in splenic DCs and macrophages. Twenty-four and 48 h after LCMV infection, spleens of *Ifna6*$^{+/GFP}$ mice were injected with 150 U/ml collagenase buffer (Wako Chemicals), 10 μg/ml DNase I (Sigma), and 10% fetal calf serum and incubated for 40 min at 37°C. After the addition of 10 mM EDTA and incubation for another 5 min, spleens were shredded and passed through a nylon mesh. Erythrocytes were lysed, and the single-cell suspension was stained with CD11b-PE, B220-PerCP, and CD11c-allophycocyanin antibodies before fluorescence-activated cell sorter analysis.

Activation of splenic DCs. Splenocytes were harvested 48 h after infection, incubated with B220-PerCP, CD11c-FITC, and CD40-, CD80-, or CD86-PE antibodies (BD Pharmingen), and analyzed by flow cytometry.

RESULTS

Impaired CTL response to LCMV infection in MyD88$^{-/-}$ mice but not IPS-1$^{-/-}$ mice. LCMV has been shown to mount a robust CTL response in vivo. Although the involvement of type I IFNs and innate immune cells in activating CTL responses has clearly been demonstrated before, the mechanism of innate recognition of LCMV in vivo is not yet fully understood. Therefore, we first examined the contributions of two major innate viral recognition systems, TLRs and RLHs, to mounting CTL responses against LCMV infection. Eight days after intravenous administration of LCMV, splenocytes of mice were harvested and stained with an H-2D^b LCMV-specific tetramer (Fig. 1A) or stimulated with gp33-41 for analysis of IFN-γ production (Fig. 1B), and total and virus-specific CD8$^+$ T lymphocytes per spleen were counted (Table 1). To assess LCMV-specific CTL activity, cells were incubated with gp33-41-loaded, ^{51}Cr-labeled EL-4 target cells and specific lysis was calculated (Fig. 1C). Wild-type mice mounted a vigorous CTL response, demonstrated by massive expansion of CD8$^+$ T cells, significant induction of LCMV-specific CD8$^+$ T cells, strong IFN-γ production,

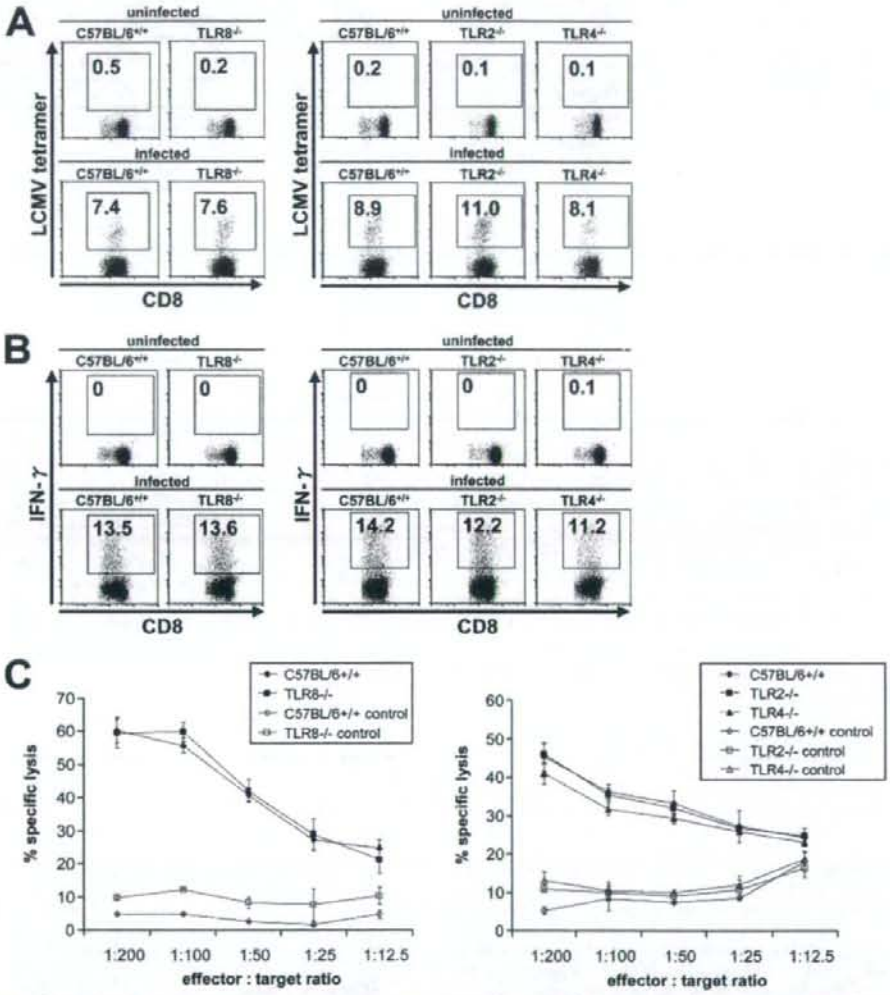

FIG. 2. Involvement of other TLRs in T-cell response. Wild-type, TLR2$^{-/-}$, TLR4$^{-/-}$, and TLR8$^{-/-}$ mice were infected intravenously with 3×10^5 PFU LCMV WE, and splenocytes were harvested on day 8 after infection. Induction of LCMV-specific T lymphocytes (A), IFN-γ production (B), and CTL activity (C) were analyzed. Values are means ± SD for three mice.

and specific, T-cell-induced lysis of >60% of labeled target cells. IFN-α/β receptor$^{-/-}$ mice and TLR7$^{-/-}$ TLR9$^{-/-}$ mice demonstrated diminished clonal expansion of cytotoxic T cells in response to LCMV infection, whereas DC8$^+$ T cells even decreased in MyD88$^{-/-}$ mice during infection compared to those in uninfected controls, resulting in splenic atrophy. Consistent with previous reports, IFN-α/β receptor$^{-/-}$ mice also showed impaired induction of LCMV-specific T cells as well as decreased IFN-γ production by these cells. Furthermore, cytotoxic T cells derived from IFN-α/β receptor$^{-/-}$ mice failed to effectively lyse target cells that presented an LCMV-specific epitope. MyD88 proved to play a crucial role in this process, as specific T-cell induction, IFN-γ production, and cytotoxicity were severely affected in MyD88$^{-/-}$ mice. In contrast, TRIF$^{-/-}$ mice did not show a defect in the activation of CD8$^+$ T cells, suggesting that TLR3 is not involved in LCMV-induced CTL responses. When mice lacking various TLRs were infected with LCMV, TLR7$^{-/-}$ TLR9$^{-/-}$ mice showed slightly diminished activation of CTL responses. In contrast, TLR2, TLR4, and TLR8 were not involved in the induction of CTL activity (Fig. 2A to C).

Next, we investigated the role of RLHs in LCMV-induced CD8$^+$ T-cell activation. The analysis of IPS-1$^{-/-}$ splenocytes revealed a normal T-cell response after LCMV infection. Specific T-cell activation, IFN-γ production, and specific lysis were comparable to those of wild-type cells (Fig. 3), suggesting that RLHs are not involved in adaptive immunity after LCMV

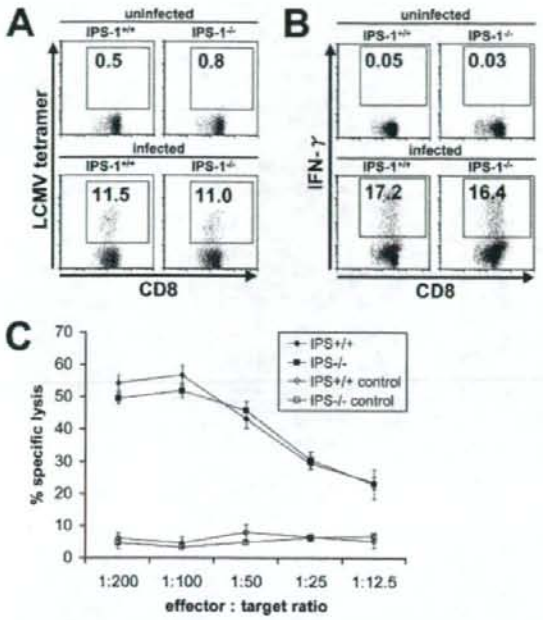

FIG. 3. T-cell response via the RLH system. Wild-type and IPS-$1^{-/-}$ mice were infected intravenously with 3×10^5 PFU LCMV WE, and splenocytes were harvested on day 8 after infection. Induction of LCMV-specific T lymphocytes (A), IFN-γ production (B), and CTL activity (C) were analyzed as described in the legend to Fig. 1. Values are means ± SD for three mice. Data are representative of three independent experiments.

infection. In general, the results obtained herein showed no difference between the WE and ARM strains of LCMV (data for LCMV ARM are not shown).

Role of TLRs and RLHs in the production of type I IFN and proinflammatory cytokines in response to LCMV infection. We further investigated how the TLR system contributes to the activation of CTL responses. Given the importance of type I IFN receptors in the development of LCMV-induced T-cell activity, we hypothesized that MyD88 is involved in the production of type I IFNs, although previous reports have shown that IFN-α production is not impaired in MyD88$^{-/-}$ mice with LCMV infection. We therefore measured serum levels of IFN-α and cytokines between 12 h and 96 h after intravenous LCMV challenge. In wild-type mice, IFN-α and IFN-β peaked 24 h after infection, and IFN-α levels gradually decreased after 48 h. IFN-α production was severely impaired in MyD88$^{-/-}$ mice (Fig. 4A), and IFN-β production was abolished (Fig. 4B), suggesting that TLRs play a critical role in type I IFN production in response to LCMV. In contrast, IFN-α production was not impaired in the absence of TRIF (data not shown), showing that TLR3 is not involved in LCMV-induced type I IFN production. Mice deficient in both TLR7 and TLR9 showed a partially impaired type I IFN response. TLR2, TLR4, and TLR8 did not play any role in the IFN response (data not shown). Thus, it is possible that a combination of TLRs might be important for the recognition of whole LCMV via MyD88 in vivo. We then investigated the involvement of RLHs by using IPS-$1^{-/-}$ mice. Although LCMV-induced IFN-α production was modestly impaired (Fig. 4A), IFN-β production was not impaired in IPS-$1^{-/-}$ mice (Fig. 4B), suggesting that the contribution of RLHs to LCMV-induced type I IFN production is smaller than that of TLRs. In general, no strain-specific differences were observed between LCMV WE and ARM infections (data for LCMV ARM are not shown).

Furthermore, we examined the levels of proinflammatory cytokines in sera. The production of IL-6, IL-12(p40), and RANTES was abolished in MyD88$^{-/-}$ mice (Fig. 5A and B). Conversely, IPS-1 deficiency did not significantly alter the production of these cytokines, suggesting that the TLR system, but not RLHs, plays an important role in the production of cytokines.

Identification of IFN-α-producing cells during LCMV infection. Previous reports pointed out that cells other than pDCs are responsible for IFN-α production during LCMV infection. Therefore, we further investigated IFN-α-producing cells in LCMV infection by using *Ifna6*$^{+/GFP}$ reporter mice. We found that 24 and 48 h after intravenous LCMV infection, GFP$^+$ cells were most frequently observed in the spleen (Fig. 6A and B) and, to a lesser extent, in inguinal lymph nodes, bone marrow, and the liver (data not shown). LCMV infection intensively increased the number of GFP$^+$ B220$^+$ CD11c^{dull} pDCs, indicating that they were the major IFN-α producers in response to LCMV infection. LCMV also modestly increased the numbers of GFP$^+$ B220$^-$ CD11c$^+$ cDCs and GFP$^+$ CD11c$^-$ CD11b$^+$ macrophages in the spleen (Fig. 6A and B), although this phenomenon was not observed in other organs (data not shown). Expression of GFP$^+$ pDCs was abolished in the absence of MyD88, whereas no significant difference was observed between wild-type and IPS-$1^{-/-}$ mice, providing evidence that pDCs utilize the TLR system to produce IFN-α. The number of GFP$^+$ cDCs and macrophages was slightly but constantly reduced in *Ifna6*$^{+/GFP}$ reporter mice lacking IPS-1 but was normal in MyD88$^{-/-}$ mice, suggesting that IFN-α production by these cell types in response to LCMV requires the RLH system and is independent of TLRs (Fig. 6A and B). Taken together, these data indicate that pDCs are the main type I IFN producers during LCMV infection through virus recognition by the TLR-MyD88 system.

Activation of DCs in response to LCMV infection. DCs have been shown to be important for the activation of adaptive immunity. One attribute of DC activation is the surface upregulation of costimulatory molecules (29). To analyze whether different DC subsets were activated in response to LCMV infections, we assessed the expression of surface CD80, CD86, and CD40 on splenic pDCs and cDCs 24 and 48 h after infection. In wild-type mice, DC expression of CD80 (Fig. 7A and B), CD86, and CD40 (data not shown) was enhanced after infection. While no differences in the induction of these surface molecules were found between wild-type and MyD88- or IPS-1-deficient cDCs, upregulation was impaired in pDCs in MyD88- but not IPS-1-deficient mice, presenting further evidence that MyD88 plays an important role in the pDC-mediated innate response to LCMV infections.

Enhanced susceptibility of MyD88$^{-/-}$ mice to LCMV infection. When wild-type mice were challenged intravenously with LCMV, the virus was cleared by the activation of CTLs, lead-

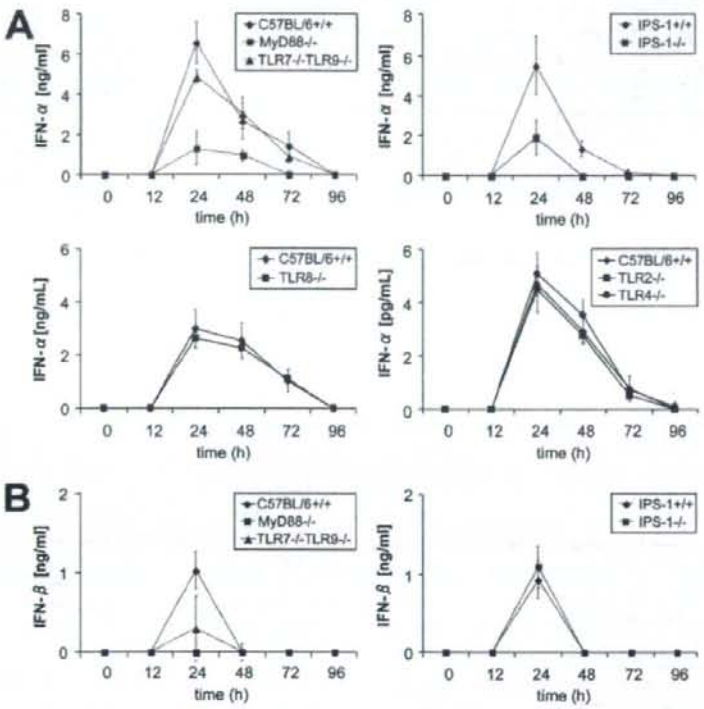

FIG. 4. Type I IFN response to LCMV infection. The indicated mice were infected intravenously with 3×10^5 PFU LCMV WE, and IFN-α (A) and IFN-β (B) levels in sera were measured by enzyme-linked immunosorbent assay between 12 and 96 h after infection. Data show means ± SD for three mice and are representative of three independent experiments.

ing to full recovery. Because MyD88$^{-/-}$ mice failed to mount a sufficient T-cell response, we further investigated the long-term outcome of LCMV infections. As expected, IPS-1$^{-/-}$ mice effectively cleared the virus from the spleen (Fig. 8B) and other organs (data not shown) within 1 week after infection, in a manner similar to that of wild-type mice. In contrast, the absence of MyD88 resulted in a failure of virus elimination, with viral titers persisting for several weeks, independent of TLR7 and TLR9 (Fig. 8A and C). This observation was in accordance with a long-lasting deficiency in T-cell function (Fig. 8E and F). The severe defects in virus clearance and in the generation of LCMV-specific T memory cells were underlined by the finding that MyD88$^{-/-}$ mice died between 30 and 40 days after challenge with higher virus titers (Fig. 8D). These results demonstrate that MyD88 is essential for the survival of mice with LCMV infection by enabling the activation of acquired immune responses.

DISCUSSION

LCMV has been studied intensively to understand the mechanisms of CTL activation following recognition of specific antigens. However, the role of innate immunity in the activation of CTL responses as well as in the elimination of the virus has yet to be clarified. When analyzing mice deficient in MyD88 or IPS-1, we clearly showed that the TLR system, but not the RLH system, is critical for the development of adaptive immunity against LCMV infection. Since the expression of IFN-α/β receptor on antigen-specific CD8$^+$ T cells is important for their expansion, activation, and memory formation after viral infection (22), the contribution of MyD88 to this process seems to be via the initial control of type I IFN production. We demonstrate that both IFN-α and IFN-β are mainly controlled by MyD88-dependent pathways. IFN-α and IFN-β share the IFN-α/β receptor for signaling, and mice deficient in IFN-α/β receptor showed impaired CTL activity during LCMV infection. Therefore, it is presumable that both IFN-α and IFN-β contribute to the generation of a CTL response to LCMV. Notably, it appears that MyD88$^{-/-}$ mice have a more severe defect in CTL responses than do IFN-α/β receptor$^{-/-}$ mice, a phenomenon also observed for CD8$^+$ T memory cells. Furthermore, IPS-1$^{-/-}$ mice did not show a defect in CTL responses, although they showed partially impaired serum IFN-α levels after LCMV infection. Thus, it is possible that the development of LCMV-specific T cells is not solely regulated by type I IFNs. In fact, at least two different pathways for LCMV-induced T-cell IFN-γ production have been described (7). Under normal conditions, the IFN-γ response is dependent on type I IFN, without a contribution of IL-12. However, mice deficient in IFN-α/β receptor elicit elevated levels of IL-12, and this may overcome the defect caused by IFN-α/β deficiency on CD8$^+$ T cells. MyD88 regulates the production of

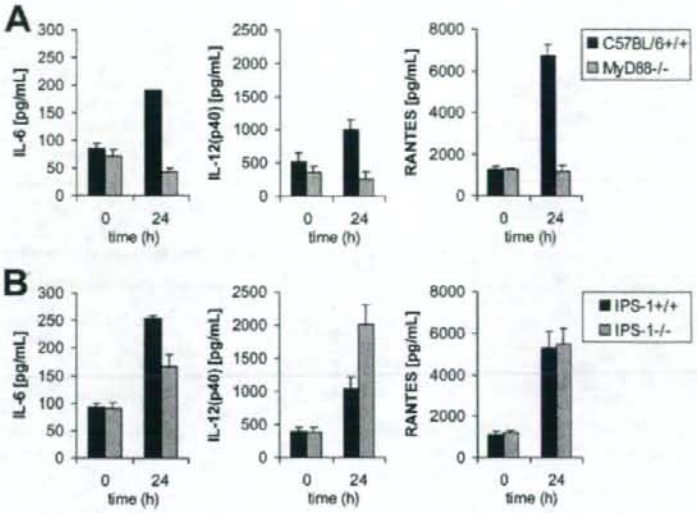

FIG. 5. Cytokine production. IL-6, IL-12(p40), and RANTES levels in sera of MyD88$^{-/-}$ (A) and IPS-1$^{-/-}$ (B) mice after intravenous infection with 3×10^5 PFU LCMV WE were assessed after 24 h by a multiplex bead-based assay. Data show means ± SD for three mice.

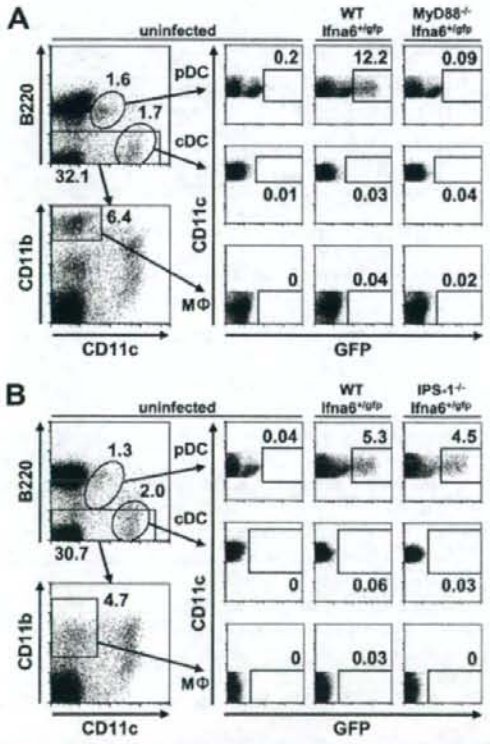

FIG. 6. Expression of GFP in splenic DCs and macrophages. *Ifna6*$^{+/GFP}$ mice lacking MyD88 (A) or IPS-1 (B) as well as wild-type mice were infected intravenously with 3×10^5 PFU LCMV WE. Splenocytes were harvested 24 and 48 h after infection, and the expression of GFP in pDCs, cDCs, and macrophages was analyzed by fluorescence-activated cell sorter analysis. Data are representative of two experiments.

various cytokines, such as IL-1, IL-6, IL-12, IL-18, and RANTES, in addition to type I IFNs, and these cytokines likely contribute to the MyD88-dependent development of LCMV-specific T cells in vivo.

Previous reports have shown that the production of type I IFNs in response to LCMV infection is not impaired in pDC-

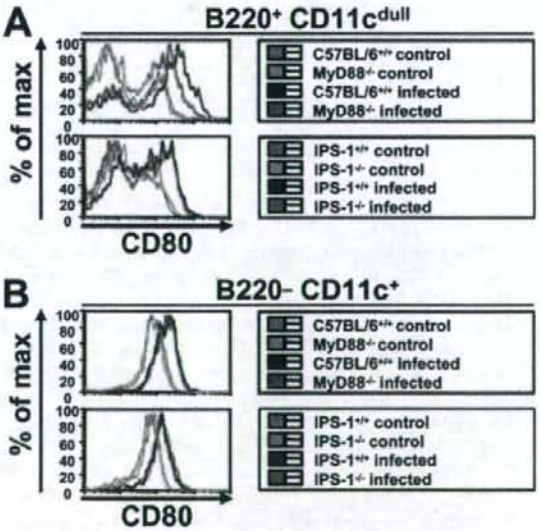

FIG. 7. Activation of splenic DCs. Mice were infected intravenously with 3×10^5 PFU LCMV WE. Splenocytes of MyD88- and IPS-1-deficient mice were investigated for the activation of CD80 on pDCs (A) and cDCs (B) by flow cytometry 48 h after infection. Data shown are representative of three mice.

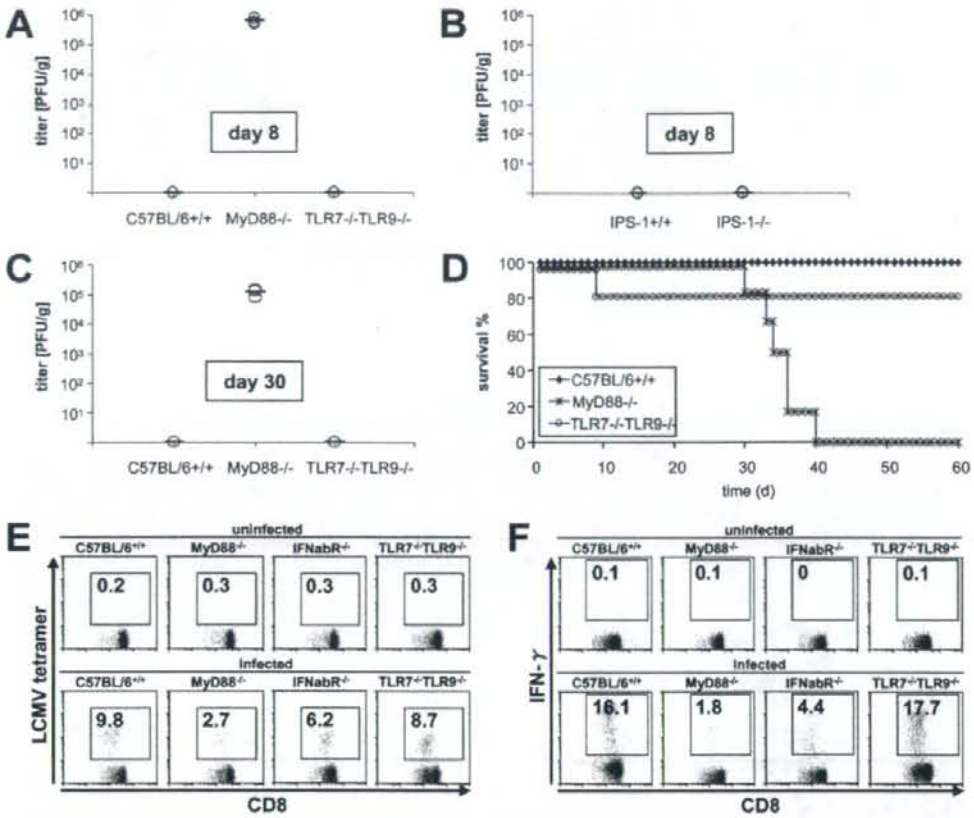

FIG. 8. Long-term sequelae after LCMV infection. Wild-type, MyD88$^{-/-}$, and TLR7$^{-/-}$ TLR9$^{-/-}$ mice or IPS-1$^{-/-}$ mice were infected intravenously with 3×10^5 PFU LCMV WE, and virus titers were measured in spleens on day 8 (A and B) and day 30 (C) by a methylcellulose titration assay. Results for three mice are displayed, with means. Data are representative of three independent experiments. (D) Survival rates were assessed after infecting six mice per indicated genotype with 2×10^6 PFU LCMV WE in two independent experiments. (E and F) Generation of LCMV-specific memory CD8$^+$ T lymphocytes in MyD88$^{-/-}$, TLR7$^{-/-}$ TLR9$^{-/-}$, and IFN-α/β receptor$^{-/-}$ mice following infection with 1×10^5 PFU LCMV WE was analyzed as described above. Indicated values are means ± SD for three mice and are representative of two independent experiments.

depleted mice (8) and that splenic cDCs from infected mice produce IFN-α (10). On the other hand, it was also suggested that splenic pDCs can produce IFN-α in response to LCMV infection (29). In this study, we identified pDCs as the predominant IFN-α producers by infecting *Ifnα6*$^{+/GFP}$ mice with LCMV. We also observed a modest expression of GFP$^+$ cDCs and macrophages in LCMV-infected reporter mice; however, this expression was clearly subordinate to that of pDCs. Other cell types, such as T and B cells, did not express GFP in early LCMV infection (data not shown), and no type I IFNs could be detected in sera later than 72 h postinfection, indicating that lymphocytes are not IFN-α producers in response to LCMV. Furthermore, we found that IFN-α production in pDCs was exclusively dependent on MyD88 but not on IPS-1. Consistently, IFN-α and IFN-β levels in sera were severely impaired in MyD88$^{-/-}$ mice. These results are in contradiction to a previous report showing that the production of type I IFNs in response to LCMV was MyD88 independent (43). Although we do not have an explanation for this discrepancy, we believe that the involvement of MyD88 as well as pDCs in the IFN response is well grounded based on the data from measurements of serum IFN and our novel reporter mice. On the other hand, cDCs and macrophages from *Ifnα6*$^{+/GFP}$ mice lacking IPS-1 showed reduced GFP expression in response to LCMV compared to those from wild-type mice, although the frequency of GFP$^+$ cells was much lower than that for pDCs. However, given that the total number of cDCs and macrophages in the body by far exceeds the number of pDCs, it can be presumed that the impaired IFN-α levels in sera in IPS-1$^{-/-}$ mice are a result of the failure to produce IFN in these cell types.

Since type I IFN production in response to LCMV infection was mainly dependent on MyD88, we investigated the contribution of each TLR to the recognition of LCMV infection. Although the involvement of TLR2 was reported previously (43), we did not detect a defect in TLR2$^{-/-}$, TLR4$^{-/-}$, or

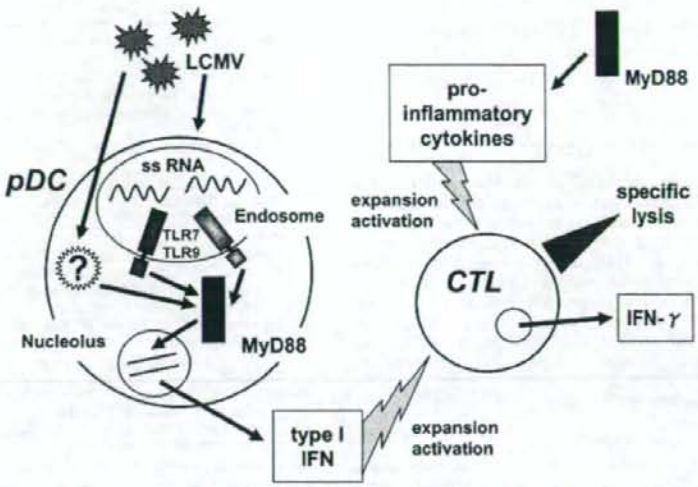

FIG. 9. Innate immune modulation of CTL response to LCMV through MyD88 signaling. MyD88 mediates recognition of LCMV by TLR7/TLR9 and possibly other, unknown receptors via pDCs. Type I IFNs produced by infected pDCs result in activation and clonal expansion of virus-specific CTLs. In an alternative pathway, CTLs are activated by proinflammatory cytokines in an MyD88-dependent manner. Activated CTLs mount effector functions that finally contribute to virus elimination.

TLR8$^{-/-}$ mice. TLR1 and TLR6 both form heterodimers with TLR2 to recognize bacterial components, and they are likely not involved in LCMV recognition, since TLR2$^{-/-}$ mice responded appropriately to LCMV infection. Also, TLR5 is unlikely to contribute to MyD88-dependent LCMV recognition, as it does not activate IFN-inducible genes and is only marginally expressed in splenic cells (37). TLR7$^{-/-}$ TLR9$^{-/-}$ mice showed only partial impairment in type I IFN levels and CTL activity compared to MyD88$^{-/-}$ mice, and TRIF was not involved in innate and adaptive immune responses to LCMV. Taken together, the data show that other unknown MyD88-dependent but TLR7- and TLR9-independent receptors may contribute to the complex orchestration of LCMV signal recognition in vivo. Another possibility is that pDCs are indirectly activated by LCMV-infected cells and that MyD88-dependent signaling is required in other cell types. Indeed, pDCs induced from bone marrow failed to produce large amounts of IFN-α in response to LCMV infection in vitro, whereas infection with Newcastle disease virus, Sendai virus, and influenza virus was reported to induce large amounts of IFN-α in bone marrow-derived pDCs (19). Thus, it is possible that IFN-α production in response to LCMV is mediated through a mechanism different from that in response to other RNA viruses. Further studies are required to clarify the mechanism of IFN-α production in pDCs via the MyD88-dependent pathway.

DCs are reported to be critical for the development of antigen-specific T-cell responses against viral infection (3). In response to LCMV infection, cDCs upregulated costimulatory molecules, namely, CD40, CD80, and CD86, even in the absence of MyD88 or IPS-1. In contrast, costimulatory molecule expression in pDCs was impaired in MyD88-deficient mice. The critical role of MyD88-dependent signaling in CD8 T-cell activation and its role in IFN production in pDCs suggested that pDCs are essential for inducing the development of LCMV-specific CTL responses. However, it is not clear if pDCs play a direct role in the presentation of LCMV antigen to CD8 T cells. A possible explanation is that pDCs act to facilitate CTL activation by producing type I IFN rather than directly presenting antigens. A model depicting the modulation of the CTL response to LCMV by pDCs via MyD88 is shown in Fig. 9.

MyD88-deficient mice were highly susceptible to infection with LCMV and showed long-lasting virus persistence. It seems that the defect in the acute-phase innate response cannot explain the cause of death observed for MyD88$^{-/-}$ mice, considering that all MyD88-deficient mice died after 30 to 40 days of infection with higher virus titers. These results are similar to the effects of LCMV infection in perforin-deficient (Perf$^{-/-}$) mice. Perf$^{-/-}$ mice have been shown to enhance T-cell expansion and activation in response to persistent LCMV infection, leading to immunomediated tissue damage and increased mortality (5, 26). Thus, it has been suggested that the pathology and fatality of LCMV infection are most likely not direct results of the infection but, rather, are due to virus-induced immunopathology. Therefore, although LCMV-mediated CTL responses, including the formation of CD8α$^+$ T memory cells, were impaired in MyD88$^{-/-}$ mice, the persistent T-cell response may eventually have caused enough pathology to result in the death of the mice. However, further studies are required to clarify the precise cause of death observed for MyD88$^{-/-}$ mice.

In summary, our results demonstrate the importance of MyD88-dependent signaling in the production of type I IFNs in pDCs. Consistently, MyD88 is critical for the activation of CTL responses. Furthermore, MyD88 controls various proinflammatory cytokines that are likely to contribute to the activation of CTL responses independently of type I IFN. However, the cell-specific contributions of TLRs and cytoplasmic

RLHs to the activation of acquired immunity appear to be different in response to various viruses. Future studies will clarify how these two innate viral recognition pathways are involved in T-cell activation depending on different viral pathogens.

ACKNOWLEDGMENTS

We thank Y. Fujiwara, M. Shiokawa, and A. Shibano for skillful technical assistance, N. Kitagaki for an excellent methodological tutorial, and P. Lee for critically reading the manuscript. M. Hashimoto deserves special appreciation for distinguished organizational support and secretarial assistance. T. Otheki kindly provided L cells and MC57G cells. EL4 cells were gratefully obtained from H. Tsutsui.

This work was supported in part by grants from the Yokochi Fund of the Kanehara Ichiro Foundation, from the Ministry of Education, Culture, Sports, Science and Technology in Japan, from the 21st Century Center of Excellence Program of Japan, and from the NIH (AI070167).

We have no competing financial interests.

REFERENCES

1. **Aichele, P., H. Unsoeld, M. Koschella, O. Schweier, U. Kalinke, and S. Vucikuja.** 2006. Cutting edge: CD8 T cells specific for lymphocytic choriomeningitis virus require type I IFN receptor for clonal expansion. J. Immunol. **176:**4525–4529.
2. **Akira, S., S. Uematsu, and O. Takeuchi.** 2006. Pathogen recognition and innate immunity. Cell **124:**783–801.
3. **Belz, G. T., K. Shortman, M. J. Bevan, and W. R. Heath.** 2005. CD8α dendritic cells selectively present MHC class I-restricted noncytological viral and intracellular bacterial antigens in vivo. J. Immunol. **175:**196–200.
4. **Beutler, B.** 2004. Interferences, questions and possibilities in Toll-like receptor signaling. Nature **230:**257–263.
5. **Binder, D., M. F. van den Broek, D. Kaegi, H. Bluethmann, J. Fehr, H. Hnegartner, and R. M. Zinkernagel.** 1989. Aplastic anemia rescued by exhaustion of cytokine-secreting $CD8^+$ T cells in persistent infection with lymphocytic choriomeningitis virus. J. Exp. Med. **187:**1902–1920.
6. **Colonna, M., A. Krug, and M. Cella.** 2002. Interferon-producing cells: on the front line in immune responses against pathogens. Curr. Opin. Immunol. **14:**373–379.
7. **Cousens, L. P., R. Peterson, S. Hsu, A. Dorner, J. D. Altman, R. Ahmed, and C. A. Biron.** 1999. Two roads diverged: interferon α/β- and interleukin 12-mediated pathways in promoting T cell interferon γ responses during viral infection. J. Exp. Med. **189:**1315–1327.
8. **Dalod, M., T. P. Salazar-Mather, L. Malmgard, C. Lewis, C. Asselin-Paturel, F. Brière, G. Trinchieri, and C. A. Brion.** 2002. Interferon α/β and interleukin 12 responses to viral infections: pathways regulating dendritic cell cytokine expression *in vivo*. J. Exp. Med. **195:**517–528.
9. **Dalod, M., T. Hamilton, R. Salomon, T. P. Salazar-Mather, S. C. Henry, J. D. Hamilton, and C. A. Biron.** 2003. Dendritic cell responses to early cytomegalovirus infection: subset functional specialization and differential regulation by interferon α/β. J. Exp. Med. **197:**885–898.
10. **Diebold, S. S., M. Montoya, H. Unger, L. Alexopoulou, P. Roy, L. E. Haswell, A. Al-Shamkhani, R. Flavell, P. Borrow, and C. Reis e Sousa.** 2003. Viral infection switches non-plasmacytoid dendritic cells into high interferon producers. Nature **424:**324–328.
11. **Gitlin, L., W. Barchet, S. Gilfillan, M. Cella, B. Beutler, R. A. Flavell, M. S. Diamond, and M. Colonna.** 2006. Essential role of MDA5 in type I IFN responses to polyriboinosinic acid and encephalomyocarditis picornavirus. Proc. Natl. Acad. Sci. USA **103:**8459–8464.
12. **Guermonprez, P., J. Valladeau, L. Zitvogel, C. Thery, and S. Amigorena.** 2002. Antigen presentation and T cell stimulation by dendritic cells. Annu. Rev. Immunol. **20:**621–676.
13. **Hemmi, H., O. Takeuchi, T. Kawai, T. Kaisho, S. Sato, H. Sanjo, M. Matsumoto, K. Hoshino, H. Wagner, K. Takeda, and S. Akira.** 2000. A Toll-like receptor recognizes bacterial DNA. Nature **408:**740–745.
14. **Hemmi, H., T. Kaisho, O. Takeuchi, S. Sato, H. Sanjo, K. Hoshino, T. Horiuchi, H. Tomizawa, K. Takeda, and S. Akira.** 2002. Small anti-viral compounds activate immune cells via the TLR7 MyD88-dependent signaling pathway. Nat. Immunol. **3:**196–200.
15. **Honda, K., H. Yanai, A. Takaoka, and T. Taniguchi.** 2005. Regulation of type I IFN induction: a current view. Int. Immunol. **17:**1367–1378.
16. **Hoshino, K., T. Kaisho, T. Iwabe, O. Takeuchi, and S. Akira.** 2002. Differential involvement of IFN-beta in Toll-like receptor-stimulated dendritic cell activation. Int. Immunol. **14:**1225–1231.
17. **Iwasaki, A., and R. Medzhitov.** 2004. Toll-like receptor control of the adaptive immune responses. Nat. Immunol. **5:**987–995.
18. **Kato, H., O. Takeuchi, S. Sato, M. Yoneyama, M. Yamamoto, K. Matsui, S. Uematsu, A. Jung, T. Kawai, O. Yamaguchi, K. Ohtsu, T. Tsujimura, C. S. Koh, C. Reis e Sousa, Y. Matsuura, T. Fujita, and S. Akira.** 2006. Differential role of MDA5 and RIG-I in the recognition of RNA viruses. Nature **141:**101–105.
19. **Kato, H., S. Sato, M. Yoneyama, M. Yamamoto, S. Uematsu, K. Matsui, T. Tsujimura, K. Takeda, T. Fujita, O. Takeuchi, and S. Akira.** 2005. Cell-type specific involvement of RIG-I in antiviral response. Immunity **23:**19–28.
20. **Kawai, T., and S. Akira.** 2006. Innate immune recognition of viral infection. Nat. Immunol. **7:**131–137.
21. **Kawai, T., K. Takahashi, S. Sato, C. Coban, H. Kumar, H. Kato, K. J. Ishii, O. Takeuchi, and S. Akira.** 2005. IPS-1, an adaptor triggering RIG-I- and MDA5-mediated type I interferon induction. Nat. Immunol. **6:**1074–1076.
22. **Kolumam, G. A., T. Sunil, L. J. Thompson, J. Sprent, and K. Murali-Krishna.** 2005. Type I interferons act directly on CD8 T cells to allow clonal expansion and memory formation in response to viral infection. J. Exp. Med. **202:**637–650.
23. **Kumagai, Y., O. Takeuchi, H. Kato, H. Kumar, K. Matsui, E. Morii, K. Aozasa, T. Kawai, and S. Akira.** 2007. Alveolar macrophages are the primary interferon-α producer in pulmonary infection with RNA viruses. Immunity **27:**240–252.
24. **Kumar, H., T. Kawai, H. Kato, S. Sato, K. Takahashi, C. Coban, M. Yamamoto, S. Uematsu, K. J. Ishii, O. Takeuchi, and S. Akira.** 2006. Essential role of IPS-1 in innate immune responses against RNA viruses. J. Exp. Med. **203:**1795–1803.
25. **Le Bon, A., and D. F. Tough.** 2002. Links between innate and adaptive immunity via type-I interferon. Curr. Opin. Immunol. **14:**432–436.
26. **Matloubian, M., M. Suresh, A. Glass, M. Galvan, K. Chow, J. K. Whitmire, C. M. Walsh, W. R. Clark, and R. Ahmed.** 1999. A role for perforin in downregulating T cell responses during chronic viral infections. J. Virol. **73:**2527–2536.
27. **Meylan, E., J. Curran, K. Hofmann, D. Moradpour, M. Binder, R. Bartenschlager, and J. Tschopp.** 2005. Cardif is an adaptor protein in the RIG-I antiviral pathway and is targeted by hepatitis C virus. Nature **437:**1167–1172.
28. **Meylan, E., J. Tschopp, and M. Karin.** 2006. Intracellular pattern recognition receptors in the host response. Nature **442:**39–44.
29. **Montoya, M., M. J. Edwards, D. M. Reid, and P. Borrow.** 2005. Rapid activation of spleen dendritic cell subsets following lymphocytic choriomeningitis virus infection of mice: analysis of the involvement of type I IFN. J. Immunol. **174:**1851–1861.
30. **Oldstone, M. B. A.** 2002. Biology and pathogenesis of lymphocytic choriomeningitis virus infection. Curr. Top. Microbiol. Immunol. **263:**83–117.
31. **Otheki, T., M. Parsons, A. Zakarian, R. G. Jones, L. T. Nguyen, J. R. Woodgett, and P. S. Ohashi.** 2000. Negative regulation of T cell proliferation and interleukin 2 production by the serine threonine kinase GSK-3. J. Exp. Med. **192:**99–104.
32. **Ou, R., S. Zhou, L. Huang, and D. Moskophidis.** 2001. Critical role for alpha/beta and gamma interferons in persistence of lymphocytic choriomeningitis virus by clonal exhaustion of cytotoxic T cells. J. Virol. **75:**8407–8423.
33. **Seth, R. B., L. Sun, C. K. Ea, and Z. J. Chen.** 2005. Identification and characterization of MAVS, a mitochondrial antiviral signaling protein that activates NF-κB and IRF3. Cell **122:**669–682.
34. **Stetson, D. B., and R. Medzhitov.** 2006. Type I interferons in host defense. Immunity **25:**373–381.
35. **Sun, Q., L. Sun, H. H. Liu, X. Chen, R. B. Seth, J. Forman, and Z. J. Chen.** 2006. The specific and essential role of MAVS in antiviral innate immune responses. Immunity **24:**633–642.
36. **Takeuchi, O., K. Hoshino, T. Kawai, H. Sanjo, H. Takada, T. Ogawa, K. Takeda, and S. Akira.** 1999. Differential roles of TLR2 and TLR4 in recognition of gram-negative and gram-positive bacterial cell wall components. Immunity **11:**443–451.
37. **Uematsu, S., M. H. Jang, N. Chevrier, Z. Guo, Y. Kumagai, M. Yamamoto, H. Kato, N. Sougawa, H. Matsui, H. Kuwata, H. Hemmi, C. Coban, T. Kawai, K. Ishii, O. Takeuchi, M. Miyasaka, K. Takeda, and S. Akira.** 2006. Detection of pathogenic intestinal bacteria by Toll-like receptor 5 on intestinal $CD11c^+$ lamina propria cells. Nat. Immunol. **7:**868–874.
38. **Uematsu, S., S. Sato, M. Yamamoto, T. Hirotani, H. Kato, F. Takeshita, M. Matsuda, C. Coban, K. Ishii, T. Kawai, O. Takeuchi, and S. Akira.** 2005. Interleukin-1 receptor-associated kinase-1 plays an essential role for Toll-like receptor (TLR)7- and TLR9-mediated interferon-α induction. J. Exp. Med. **201:**915–923.
39. **Xu, L. G., Y. Y. Wang, K. J. Han, L. Y. Li, Z. Zhai, and H. B. Shu.** 2005. VISA is an adaptor protein required for virus-triggered IFN-β signaling. Mol. Cell **19:**727–740.
40. **Yamamoto, M., S. Sato, H. Hemmi, K. Hoshino, T. Kaisho, H. Sanjo, O. Takeuchi, M. Sugiyama, M. Okabe, K. Takeda, and S. Akira.** 2003. Role of adaptor TRIF in the MyD88-independent Toll-like receptor signaling pathway. Science **301:**640–643.
41. **Yoneyama, M., M. Kikuchi, K. Matsumoto, T. Imaizumi, M. Miyagishi, K.**

Taira, E. Foy, Y. M. Loo, M. Gale, S. Akira, S. Yonehara, A. Kato, and T. Fujita. 2005. Shared and unique functions of the DExD/H-box helicases RIG-I, MDA5, and LGP2 in antiviral innate immunity. J. Immunol. **175:** 2851–2858.

42. **Yoneyama, M., M. Kikuchi, T. Natsukawa, N. Shinobu, T. Imaizumi, M. Miyagishi, K. Taira, S. Akira, and T. Fujita.** 2004. The RNA helicase RIG-I has an essential function in double-stranded RNA-induced innate antiviral responses. Nat. Immunol. **5:**730–737.
43. **Zhou, S., E. A. Kurt-Jones, L. Mandell, A. Cerny, M. Chan, D. T. Golenbock, and R. W. Finberg.** 2005. MyD88 is critical for the development of innate and adaptive immunity during acute lymphocytic choriomeningitis virus infections. Eur. J. Immunol. **35:**822–830.

Published June 30, 2008

JEM

ARTICLE

Length-dependent recognition of double-stranded ribonucleic acids by retinoic acid–inducible gene-I and melanoma differentiation–associated gene 5

Hiroki Kato,[1,2] Osamu Takeuchi,[1,2] Eriko Mikamo-Satoh,[3,4] Reiko Hirai,[5] Tomoji Kawai,[3] Kazufumi Matsushita,[1,2] Akane Hiiragi,[6] Terence S. Dermody,[7] Takashi Fujita,[5,6] and Shizuo Akira[1,2]

[1]Laboratory of Host Defense, World Premiere International Immunology Frontier Research Center, [2]Research Institute for Microbial Diseases, [3]Institute for Scientific and Industrial Research, Osaka University, Suita, Osaka 565-0871, Japan
[4]Department of Pharmacy, Hyogo University of Health Sciences, Cyuo-ku, Kobe, Hyogo 650-8530, Japan
[5]Laboratory of Molecular Genetics, Institute for Virus Research, and [6]Laboratory of Molecular Cell Biology, Graduate School of Biostudies, Kyoto University, Kyoto 606-8502, Japan
[7]Department of Pediatrics, Vanderbilt University School of Medicine, Nashville, TN 37232

The ribonucleic acid (RNA) helicases retinoic acid–inducible gene-I (RIG-I) and melanoma differentiation–associated gene 5 (MDA5) recognize distinct viral and synthetic RNAs, leading to the production of interferons. Although 5′-triphosphate single-stranded RNA is a RIG-I ligand, the role of RIG-I and MDA5 in double-stranded (ds) RNA recognition remains to be characterized. In this study, we show that the length of dsRNA is important for differential recognition by RIG-I and MDA5. The MDA5 ligand, polyinosinic-polycytidylic acid, was converted to a RIG-I ligand after shortening of the dsRNA length. In addition, viral dsRNAs differentially activated RIG-I and MDA5, depending on their length. Vesicular stomatitis virus infection generated dsRNA, which is responsible for RIG-I–mediated recognition. Collectively, RIG-I detects dsRNAs without a 5′-triphosphate end, and RIG-I and MDA5 selectively recognize short and long dsRNAs, respectively.

CORRESPONDENCE
Shizuo Akira:
sakira@biken.osaka-u.ac.jp

Abbreviations used in this paper: AFM, atomic force microscope; CARD, caspase-recruitment domain; cDC, conventional DC; CIAP, calf intestine alkaline phosphatase; DI, defective interfering; dsRNA, double-stranded RNA; EMCV, encephalomyocarditis virus; IPS-1, IFN-β stimulator-1; MEF, mouse embryonic fibroblast; MDA5, melanoma differentiation–associated gene 5; pDC, plasmacytoid DC; PNPase, polynucleotide phosphorylase; poly I:C, polyinosine-polycytidylic acid; PRR, pattern recognition receptor; RIG-I, retinoic acid-inducible gene-I; RLH, RIG-I–like helicase; ssRNA, single-stranded RNA; TIR, Toll/IL-1 receptor homology; TLR, Toll-like receptor; VSV, vesicular stomatitis virus.

The first line of defense against RNA virus infection relies on the innate immune system, which is initiated by the detection of viral components. Sensing of pathogens by innate immunity is mediated by host pattern recognition receptors (PRRs) that detect pathogen-specific molecular patterns (1). Three different classes of PRRs have been identified: Toll-like receptors (TLRs), retinoic acid–inducible gene-I (RIG-I)–like helicases (RLHs), and NOD-like receptors (2–4). The recognition of viruses by the PRRs leads to production of proinflammatory cytokines and type I IFNs. In particular, type I IFNs, comprised of multiple IFN-αs and -βs, are important for eliminating invading viruses by inducing death of infected cells, conferring resistance to viral infection on surrounding cells, and activating acquired immune responses.

Among PRRs, TLRs and RLHs are known to recognize viral infection. TLRs are transmembrane receptors with leucine-rich repeats and a cytoplasmic Toll/IL-1 receptor homology (TIR) domain. TLR3, 7, and 9 are located on endosome/ER membranes, and detect double-stranded (ds) RNA, single-stranded (ss) RNA, and DNA with a CpG motif, respectively (5–8). Upon encountering their cognate ligands, TLRs activate intracellular signaling cascades by recruiting the TIR domain containing adaptor molecules, such as MyD88 and TRIF (9, 10). Ultimately, the signaling leads to the expression of type I IFNs and proinflammatory cytokine genes. TLR7 and 9 are highly expressed on plasmacytoid DCs (pDCs), a cell type known to produce vast amounts of type I IFNs in response to viral infection (11). The importance of TLRs in the production of type I IFNs in pDCs have been shown by using mice deficient in MyD88, which is responsible for TLR7 and 9 signaling.

However, TLRs are dispensable for virus-induced IFN production in cell types other than pDCs. Instead, RIG-I family cytoplasmic

The online version of this article contains supplemental material.

Published June 30, 2008

RNA helicases play a key role in sensing RNA virus invasion. The RIG-I family consists of three helicases, RIG-I, melanoma-di erentiation–associated gene 5 (MDA5), and LGP2 (12–14). RIG-I and MDA5 contain two caspase-recruitment domains (CARDs) and a DExD/H-box helicase domain. The helicase domains of RIG-I and MDA5 recognize viral RNAs, and their CARDs are responsible for signaling through interacting with a CARD-containing adaptor, IFN-β promoter stimulator-1 (IPS-1) (15, 16), also called MAVS, CARDIF, and VISA (17–20), which is located in the outer mitochondrial membrane. This interaction nally activates several transcriptional factors, IFN regulator factor 3, IFN regulator factor 7, and NF-κB for the induction of type I IFNs and proin ammatory cytokines (21, 22). In contrast, LGP2 does not possess a CARD, but only a DExD/H-box helicase domain, and has been reported to function as a negative regulator (14, 23), especially of the RIG-I–mediated pathway (24, 25).

Recent studies have demonstrated that RIG-I and MDA5 are di erentially involved in antiviral responses. Picornaviruses, such as encephalomyocarditis virus (EMCV), are speci cally recognized by MDA5, whereas RIG-I recognizes a wide variety of RNA viruses belonging to the paramyxovirus and rhabdovirus families, as well as Japanese encephalitis virus (26). Some viruses such as Dengue virus and reovirus were shown to be recognized by both RIG-I and MDA5 (27). These two helicases have also been shown to recognize distinct types of RNAs. Single-stranded (ss) RNA with 5′-triphosphate has been identi ed as a RIG-I ligand (26, 28–30). The cellar 5′-triphosphate ssRNA does not exist in the cytoplasm, but in the nucleus, and ssRNAs in the cytoplasm are normally capped or processed. Thus, RIG-I can distinguish viral RNAs from vast amounts of cellar RNAs. On the other hand, small dsRNAs (ranging from 21 to 27 nucleotides) have also been reported to induce IFN-inducible genes via both ATPase and helicase activities of RIG-I (31).

However, whether or not dsRNA is also a RIG-I ligand, in addition to 5′-triphosphate ssRNA, is still controversial. Although polyinosinic-polycytidylic acid (poly I:C), an arti cial double-stranded (ds) RNA, was found to be a ligand for MDA5 (26, 28), the motif recognized by MDA5 should be characterized, and a natural ligand for MDA5 is also yet to be discovered.

In this study, we investigated how RIG-I and MDA5 di erentially recognize RNAs by chemically modifying poly I:C. We found that the MDA5 ligand, poly I:C, was converted to a RIG-I ligand after shortening of the dsRNA length. RIG-I and MDA5 preferentially bind to short and long poly I:Cs, respectively. In addition, dsRNAs prepared from viruses di erentially activated RIG-I and MDA5, depending on the length. Whereas in uenza virus infection failed to generate dsRNA in the infected cells, vesicular stomatitis virus (VSV) infection generated dsRNA, which is responsible for RIG-I–mediated recognition. Collectively, RIG-I detects dsRNAs without a 5′-triphosphate end, and RIG-I and MDA5 selectively recognize short and long dsRNAs, respectively.

RESULTS

The switching of poly I:C from an MDA5 ligand to a RIG-I ligand

We rst estimated the length of the MDA5 ligand poly I:C by agarose gel electrophoresis and found that untreated poly I:C migrated as a smeared band corresponding to the mobility of 4–8 kbp dsDNA fragments (Fig. 1 A). To analyze the importance of poly I:C length in IFN-inducing activity, we partially digested poly I:C with a dsRNA-speci c endonuclease, RNase III. The size of the poly I:C became shorter in a digestion time-dependent manner, and the median size of 60 min–treated poly I:C corresponded to 300 bp dsDNA (Fig. 1 A). When WT, *Rig-I*$^{-/-}$, *Mda5*$^{-/-}$, *Rig-I*$^{-/-}$*Mda5*$^{-/-}$ mouse embryonic broblasts (MEFs) were stimulated with untreated poly I:C, IFN-β was induced in an MDA5-dependent manner that was consistent with previous reports (26, 28). Surprisingly, IFN-β induction by poly I:C treated with RNase III for 60 min depended on RIG-I, but not on MDA5 (Fig. 1 B). However, complete digestion of poly I:C by 180-min treatment with RNase III produced 10–20 nt dsRNA that failed to activate even wild-type cells (Fig. 1 B and unpublished data). When cells were stimulated with poly I:C partially digested for di erent periods, *Mda5*$^{-/-}$ MEFs gained the ability to respond to RNase III–treated poly I:C as the digestion proceeded, whereas *Rig-I*$^{-/-}$ MEFs gradually lost the ability to produce IFN-β in response to shortened poly I:C (Fig. 1 C). In addition, conventional DCs derived from bone marrow or prepared from spleen from *Rig-I*$^{-/-}$ and *Mda5*$^{-/-}$ mice also

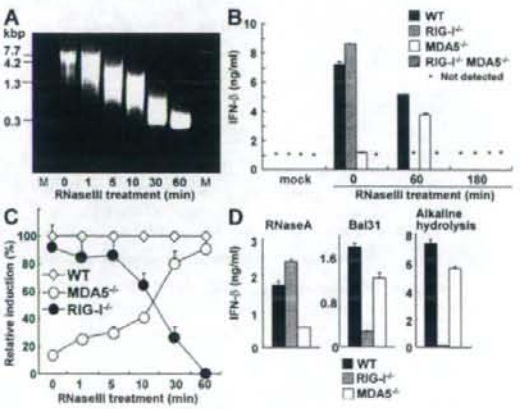

Figure 1. Preferential recognition of long and short poly I:C by MDA5 and RIG-I. (A) The indicated RNAs are shown on the ethidium bromide–stained agarose gel. M, DNA marker. (B) WT, *Rig-I*$^{-/-}$, *Mda5*$^{-/-}$, and *Rig-I*$^{-/-}$*Mda5*$^{-/-}$ MEFs were treated with 1 μg/ml of untreated or RNase III–treated poly I:C for 16 h. The production of IFN-β in the supernatant was measured by ELISA. mock, no RNA. (C) Relative induction of IFN-β after stimulation with poly I:C treated with RNase III for the indicated periods. (D) The production level of IFN-β in the stimulation with RNase A–treated, Bal31-treated, or alkaline-hydrolyzed poly I:C. Error bars show the SDs between triplicates.

Published June 30, 2008

failed to produce IFN-β in response to RNase III–digested and undigested poly I:C, respectively (Fig. S1, available at http://www.jem.org/cgi/content/full/jem.20080091/DC1). Furthermore, production of IFN-β in the sera in response to digested and undigested poly I:C conjugated with a transfection reagent was dependent on the presence of RIG-I and MDA5, respectively (Fig. S2). These results indicate the switching of poly I:C from being an MDA5 ligand to being a RIG-I ligand after partial digestion with RNase III.

Poly I:C partially digested with human Dicer also induced IFN-β in a RIG-I–dependent manner (unpublished data), indicating that this phenomenon is not speci c to bacterial RNase III. In contrast, digestion of poly I:C with a ssRNA-speci c nuclease, RNase A, did not a ect its recognition by MDA5 (Fig. 1 D), suggesting that the shortening of the dsRNA part of poly I:C is necessary for the conversion from an MDA5 ligand to a RIG-I ligand. Consistent with the aforementioned observations, treatment with Bal 31, which degrades ssRNA and linear duplex RNA progressively from both the 5′- and 3′-ends, as well as alkaline hydrolysis, also converted poly I:C to a RIG-I ligand (Fig. 1 D). Poly I:C is an arti cial dsRNA generated by annealing poly I and poly C. Poly I and C are synthesized by a bacterial enzyme, polynucleotide phosphorylase (PNPase), which catalyzes the polymerization of nucleotide diphosphate (32). Because poly I and C are synthesized with inositol diphosphate and cytidine diphosphate as substrates, poly I:C does not contain a 5′-triphosphate nucleotide, and dsRNA fragments generated by RNase III digestion contain a 5′-monophosphate end, showing absence of triphosphates in the prepared poly I:C solution. Furthermore, IFN induction by poly I:C treated with RNase III for 60 min was not altered by additional treatment with RNase A for the removal of ssRNA contamination (unpublished data), indicating that RIG-I recognizes dsRNA without triphosphates, in addition to 5′-triphosphate ssRNAs. Collectively, these results suggest that the length of poly I:C determines the di erential recognition by RIG-I and MDA5.

Differential regulation of ATPase activity by long and short poly I:C

It has been shown that RIG-I has the ability to catalyze ATP in the presence of dsRNA. To determine if this ATPase activity of these helicases is di erentially activated by dsRNAs in a length-dependent manner, we examined the ATPase activity of puri ed RIG-I and MDA5 proteins in the presence of poly I:C or poly I:C treated with RNase III for 60 min (designated as short poly I:C). The ATPase activity of RIG-I increased in the presence of short poly I:C in a dose-dependent manner, and the activation was higher than that with untreated poly I:C. In contrast, untreated poly I:C strongly activated the ATPase activity of MDA5 compared with short poly I:C (Fig. 2 A), indicating that the ATPase activities of RIG-I and MDA5 are selectively activated by the short poly I:C and untreated long poly I:C, respectively. As expected, 5′-triphosphate ssRNA induced the ATPase activity of RIG-I, but not of MDA5 (Fig. 2 B). Thus, the ATPase activity clearly correlated with the IFN responses triggered by these RNA helicases, indicating that RIG-I and MDA5 directly distinguish between short and untreated long poly I:C molecules, respectively.

Association of poly I:C with RIG-I and MDA5

To investigate whether RIG-I and MDA5 directly distinguish between the lengths of poly I:C, we examined the binding of puri ed RIG-I and MDA5 proteins to poly I:C by atomic force microscope (AFM). As shown in Fig. 3 A, untreated poly I:C was detected as strings with lengths of 100–200 nm, and short poly I:C was visualized as dots (1 nm high). MDA5 mixed with untreated poly I:C formed a thick structure indicated by bright white dots, representing the binding between MDA5 and poly I:C (Fig. 3 A). On the other hand, the mixture of RIG-I and untreated poly I:C failed to form such complexes. Reciprocally, short poly I:C mixed with RIG-I, but not MDA5, formed the thick structures. Next, we statistically analyzed the thickness of molecules visualized by AFM. Whereas the heights of poly I:C, short poly I:C, MDA5, or RIG-I alone were 0.5–1.5 nm, 2.5–5.5 nm structures appeared when poly I:C was mixed with MDA5, but not with RIG-I, protein (Fig. 3 B). In contrast, as shown in Fig. 3 C, an association of short poly I:C with RIG-I, but not with MDA5, was detected. These data indicate that RIG-I and MDA5 distinguish the lengths of poly I:C and speci cally bind to their cognate ligands.

Differential recognition of short and long dsRNAs by two helicases

We examined if short dsRNAs other than poly I:C are also recognized by RIG-I. We chemically synthesized 70 base sense and antisense ssRNAs corresponding to the sequence of Lamin A/C harboring a 5′ hydroxyl end, annealed them, and examined their IFN-inducing ability. Whereas transfection of ssRNAs did not induce production of IFN-β, dsRNA generated by annealing sense and antisense ssRNAs (designated s and as in Fig. 4 A) induced IFN-β. Although the level of production was comparably low, it was clearly

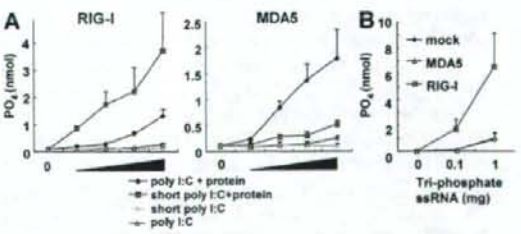

Figure 2. Long and short poly I:C preferentially activate ATPase activities of MDA5 and RIG-I. ATPase activity of RIG-I or MDA5 protein was measured in the presence of the indicated RNAs. The x axis shows the concentration of RNAs. (A) Long and short poly I:C. (B) 5′-tri-phosphate ssRNA. Several quantities (1, 0.2, 0.04, and 0.008 µg) of poly I:C were used. Error bars show SDs between triplicates.

Published June 30, 2008

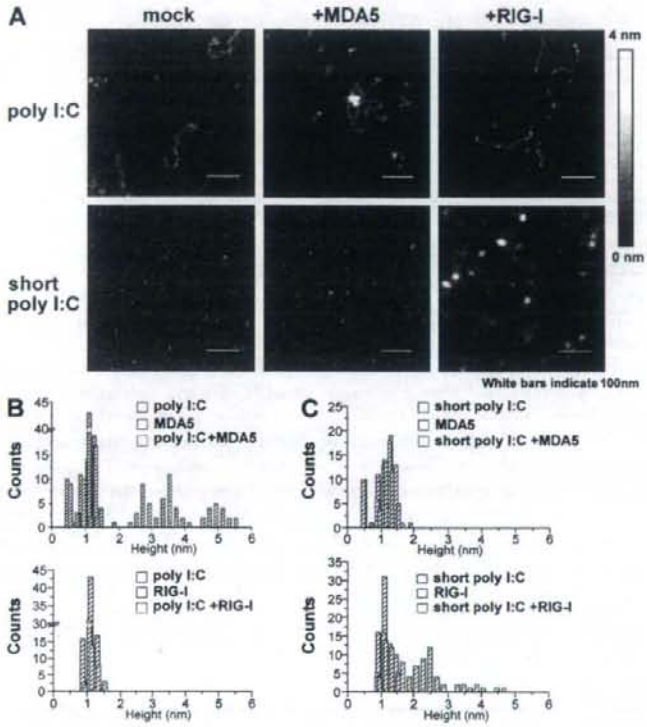

Figure 3. RIG-I and MDA5 specifically bind to short and long poly I:C. (A) Complex of indicated poly I:C and protein (MDA5 or RIG-I) was observed by AFM. Height is on a scale from 0 to 4 nm, with a low area depicted in dark brown and a higher area depicted in brighter color. Scale area, 500 nm. Bars, 100 nm. Those are representative images from several pictures. (B and C) Statistical height analyses of molecules corresponding to pictures in A.

dependent on RIG-I, indicating that a 70-bp dsRNA without 5′ triphosphate is also a RIG-I ligand (Fig. 4 A). To further analyze longer dsRNA synthesized in vitro by T7 polymerase in the production of IFN-β, we generated a 400 base sense and antisense ssRNA corresponding to the sequence of Lamin A/C harboring a 5′ capping with 7mG (designated s and as in Fig. 4 B). Introduction of dsRNA, generated by annealing capped 400 base sense and antisense ssRNAs, induced greatly enhanced RIG-I–dependent IFN-β production compared with the transfection of cells with each ssRNA (Fig. 4 B). These data also supported the aforementioned observation that dsRNA can induce IFN responses in a RIG-I–dependent fashion. We further examined the IFN responses triggered by 1–4 kbp capped-dsRNA. Although 1 kbp dsRNA-induced IFN-β was dependent on RIG-I, but not on MDA5, 2 kbp capped-dsRNA induced IFN-β, even in *Rig-I*$^{-/-}$ cells. The production of IFN-β in response to 3 and 4 kbp capped-dsRNA was less dependent on RIG-I, and an impairment of IFN-β production was observed in *Mda5*$^{-/-}$ cells (Fig. 4 C). Of note, *Rig-I*$^{-/-}$ *Mda5*$^{-/-}$ cells did not produce any IFN-β in response to 1–4 kbp capped-dsRNA (Fig. 4 C). These data indicate that RIG-I and MDA5 preferentially recognize short and long dsRNAs synthesized by T7 polymerase, respectively.

Recognition of viral genomic dsRNA by RIG-I and MDA5

We then examined whether viral dsRNAs are also di erentially recognized by RIG-I and MDA5. Reovirus, a dsRNA virus, was used for further analysis. The production of IFN-β in response to reovirus was severely impaired in *Mda5*$^{-/-}$ conventional DCs (cDCs; Fig. 5 A), although this was totally abolished in *Rig-I* $^{-/-}$ *Mda5*$^{-/-}$ cDCs (not depicted). This result indicates that both RIG-I and MDA5 are involved in the recognition of reovirus, which is consistent with a recent study (24). Next, we stimulated MEFs with whole genomic RNA prepared from reovirus. Reovirus genome RNA induced production of IFN-β in either *Rig-I* $^{-/-}$ cells or *Mda5*$^{-/-}$ MEFs, but not in *Rig-I* $^{-/-}$ *Mda5*$^{-/-}$ MEFs (Fig. 5 B). These ndings suggest that the reovirus genome RNA contains both RIG-I and MDA5 ligands. Reovirus genome RNA consists of 10 segments in three distinct classes called L, M, and S corresponding to their size. Segment sizes are 3.9 kbp (L), 2.2–2.3 kbp (M), and 1.2–1.4 kbp (S; Fig. 5 C). These fragments were puri ed from the whole reovirus genome and each fragment

Published June 30, 2008

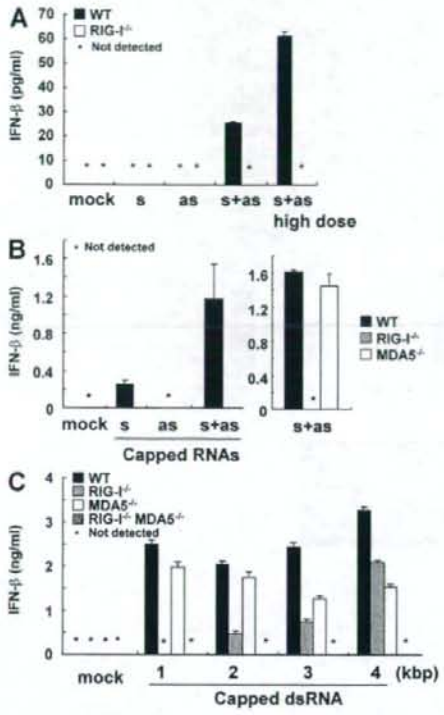

Figure 4. RIG-I and MDA5 selectively recognize dsRNA in a length-dependent manner. (A and B) Indicated genotype of MEFs were treated with 1 μg/ml of the indicated RNAs (10 μg/ml in the case of high dose) for 24 h. s, sense ssRNA; as, antisense ssRNA; s+as, dsRNA generated by annealing s with as. s and as are chemically synthesized 70-bp ssRNAs having a 5′ hydroxyl end in A. s and as are in vitro transcribed capped-ssRNAs in (B). The production of IFN-β in the supernatant was measured by ELISA. (C) WT, *Rig-I*$^{-/-}$, *Mda5*$^{-/-}$, and *Rig-I*$^{-/-}$ *Mda5*$^{-/-}$ MEFs were treated with 1 μg/ml of in vitro–transcribed capped dsRNAs for 16 h. The production of IFN-β in the supernatant was measured by ELISA. Error bars show SDs between triplicates.

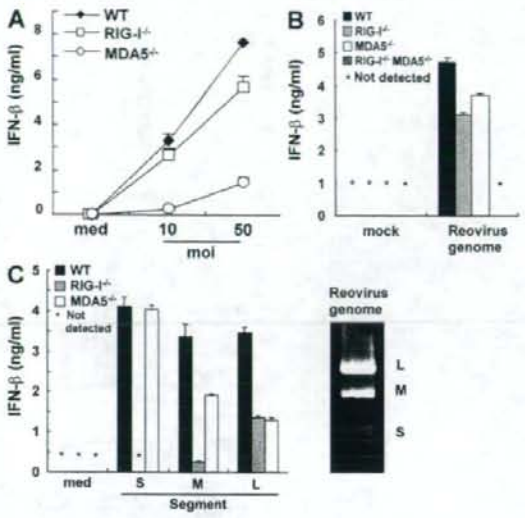

Figure 5. Reovirus genome dsRNA includes both RIG-I and MDA5 ligands. (A) WT, *Rig-I*$^{-/-}$, and *Mda5*$^{-/-}$ GM-CSF-DCs were infected with the indicated multiplicity of infection of reovirus. The production of IFN-β in the supernatant was measured by ELISA. (B and C) The indicated genotypes of MEFs were treated with 1 μg/ml of reovirus genome RNA (B) or 0.1 μg/ml of dsRNA segments (C) for 16 h. The production of IFN-β in the supernatant was measured by ELISA. The reoviral genome is shown on the ethidium bromide–stained gel (C, right), and the S (1.2–1.4 kbp), M (2.2–2.3 kbp), and L (3.9 kbp) segments are indicated. Error bars show SDs between triplicates.

was separately transfected into MEFs. As shown in Fig. 5 C, the production of IFN-β in response to S segments was dependent on RIG-I, but not on MDA5. The response to M fragments was not abrogated in *Rig-I*$^{-/-}$ MEFs, and was modestly impaired in *Mda5*$^{-/-}$ MEFs. In contrast, the production of IFN-β induced by L segments was reduced in both *Rig-I*$^{-/-}$ and *Mda5*$^{-/-}$ MEFs, suggesting that MDA5 contributed more to the recognition of longer segments of reovirus genomic dsRNA, whereas shorter segments were preferentially recognized by RIG-I.

MDA5 and RIG-I recognize viral dsRNA generated during replication

We have reported that EMCV is recognized by MDA5, whereas RIG-I detects VSV and in uenza virus. In response to in uenza virus infection, triphosphate ssRNA was considered to be the source of induction of type I IFNs, and no dsRNA was detectable during its replication (30, 33). To investigate whether triphosphate ssRNA is also the source of type I IFN induction in VSV infection, we harvested whole RNA from noninfected cells or virus-infected cells, and examined the IFN-β responses to the RNAs. RNA prepared from EMCV-infected cells induced IFN-β production in an MDA5-dependent manner (Fig. 6 A). Treatment of this RNA with calf intestine alkaline phosphatase (CIAP) did not reduce IFN-β production in MEFs (Fig. 6 B). In contrast, RNA from in uenza virus-infected cells induced IFN-β production in a RIG-I–dependent manner, which was severely reduced after CIAP treatment (Fig. 6, A and B). IFN-β production in response to RNA from VSV-infected cells was dependent on RIG-I (Fig. 6 A) and this production was only partially reduced by treatment with CIAP (Fig. 6 B). These data suggest that 5′-triphosphate ssRNA is not the sole RIG-I ligand involved in VSV-induced IFN-β production. Furthermore, degradation of dsRNA from virus-infected cells by RNase III treatment abolished IFN-β–inducing activity in RNA from EMCV-infected cells (Fig. 6 B). Also the level of IFN production was impaired in RNA from VSV-infected cells by RNase III treatment, whereas the response to RNA from

Published June 30, 2008

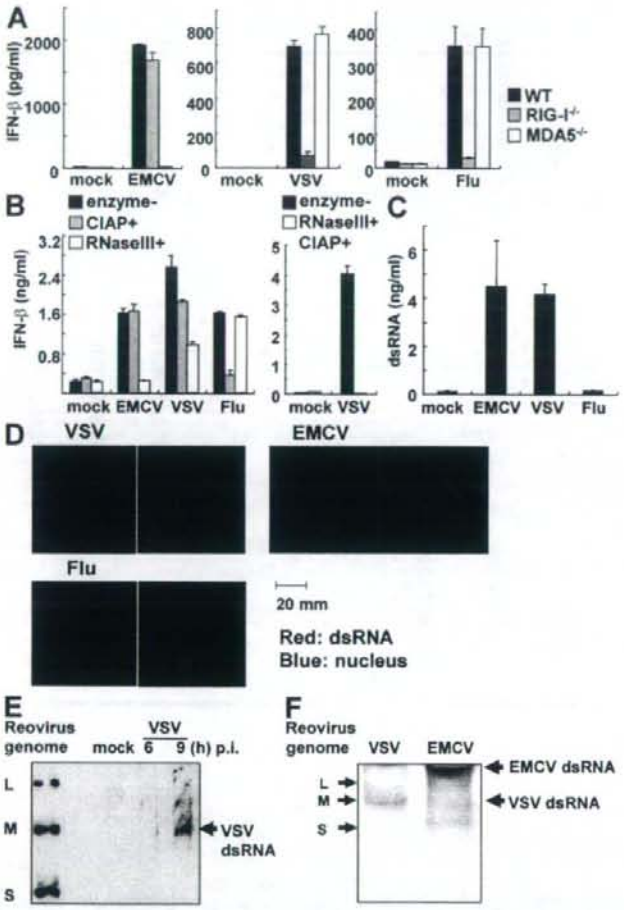

Figure 6. dsRNA generated during VSV replication induces IFNs in a RIG-I–dependent manner. (A) RNA samples harvested from uninfected (mock), EMCV-, VSV-, or influenza virus (flu)–infected cells were transfected into WT, *Rig-I*$^{-/-}$, and *Mda5*$^{-/-}$ MEFs. The production of IFN-β in the culture supernatant 10 h after transfection was measured by ELISA. (B) RNA harvested from noninfected (mock) or EMCV-, VSV-, or influenza virus–infected cells with CIAP-, RNase III-, both CIAP-, and RNase III-treatments or nontreatment (enzyme-) was transfected into WT MEFs. The production of IFN-β in the supernatant 10 h after transfection was measured by ELISA. (C) dsRNA in uninfected (mock), EMCV-, VSV-, or influenza virus-infected cells was measured by ELISA. (D) Immunostaining for dsRNA in MEFs infected with EMCV, VSV, and influenza virus for 8 h. Red, dsRNA; blue, nucleus. Error bars show SDs between triplicates. (E) RNA harvested from noninfected (mock) or VSV-infected cells (indicated periods) was electrophoresed in 1.5% agarose gel, transferred to a nylon membrane, and blotted by anti-dsRNA antibody. Reovirus genome RNAs were indicated as the size control. The arrow shows VSV dsRNA. (F) dsRNA blotting of RNA harvested from EMCV- or VSV-infected cells. RNAs were electrophoresed in nondenaturing 10% polyacrylamide gel. Reovirus genome RNAs were indicated (left). Arrows (right) show EMCV and VSV dsRNA.

in uenza virus-infected cells was not altered after treatment. Moreover, treatment of RNA from VSV-infected cells with both CIAP- and RNase III abolished IFN-β–inducing activity (Fig. 6 B). These results further suggest that the dsRNA generated in VSV-infected cells is recognized by RIG-I to induce IFN-β production. To determine if dsRNA is generated during VSV infection, we performed quanti cation of dsRNA in viral-infected cells by ELISA. Interestingly, infection with VSV and EMCV produced high amounts of dsRNA, despite no dsRNA being detected after infection with in uenza virus (Fig. 6 C). As shown in Fig. 6 D, dsRNA (red dot) was observed in EMCV-infected cells, but not in in uenza virus-infected cells, consistent with previous reports (30, 33). The presence of dsRNA was also detected in VSV-infected cells (Fig. 6 D). These results suggest that dsRNA is generated in cells infected with VSV, a virus recognized by RIG-I,